AMRL-TR-65-66

AD Le 30 296
Utation

ELECTRON MICROSCOPIC AND MORPHOMETRIC STUDY OF RATS EXPOSED TO 98.5 PERCENT OXYGEN AT ATMOSPHERIC PRESSURE

GONZAGUE S. KISTLER, MD

UNIVERSITY OF ZURICH

PETER R. B. CALDWELL, CAPTAIN, MC, USAF

AEROSPACE MEDICAL RESEARCH LABORATORIES

EWALD R. WEIBEL, MD

UNIVERSITY OF ZURICH

DECEMBER 1965

AEROSPACE MEDICAL RESEARCH LABORATORIES
AEROSPACE MEDICAL DIVISION
AIR FORCE SYSTEMS COMMAND
WRIGHT-PATTERSON AIR FORCE BASE, OHIO

ELECTRON MICROSCOPIC AND MORPHOMETRIC STUDY OF RATS EXPOSED TO 98.5 PERCENT OXYGEN AT ATMOSPHERIC PRESSURE

GONZAGUE S. KISTLER, MD

PETER R. B. CALDWELL, CAPTAIN, MC, USAF

EWALD R. WEIBEL, MD

FOREWORD

This study was initiated by the Biomedical Laboratory of the Aerospace Medical Research Laboratories, Aerospace Medical Division, Wright-Patterson Air Force Base, Ohio. The research was conducted by the Department of Anatomy, University of Zurich, Zurich, Switzerland, under Contract AF 61(052)-784, through the European Office of Aerospace Research (OAR), United States Air Force. Captain Peter R.B. Caldwell, MC, initiated the contract, Captain Philip Felig, MC, and Major E.R. Archibald, MSC, of the Altitude Protection Branch, Physiology Division were the contractor monitors for the Aerospace Medical Research Laboratories. The work was performed in support of Project 7164, "Biomedical Criteria for Aerospace Flight," Task 716404, "Physiological Criteria for Altered Environments." This report covers research performed between February 1964 and July 1965.

The authors gratefully acknowledge the technical support of the enlisted personnel at Aerospace Medical Research Laboratories, under the direction of SMSgt J.B. Graves; Mr. W. O. Butler of the Miami Valley Hospital Research Department, Dayton, Ohio; and Mr. W. Scherle, Miss E. Amrein, Miss J. Meier, Mrs. G. Fondren, and Miss M. Manuel, of the Anatomisches Institute in Zurich. The electron microscope facilities used were provided by the Swiss National Science Foundation.

This technical report has been reviewed and is approved.

WAYNE H. McCANDLESS
Technical Director
Biomedical Laboratory
Aerospace Medical Research Laboratories

ABSTRACT

Rats were exposed to 98.5% oxygen at 765 Torr in a controlled environmental chamber. Groups were sacrificed at 6, 24, 48, and 72 hours and the lungs were prepared for light and electron microscopic examination. A control group breathed room air. In the groups which breathed oxygen for 6 and 24 hours no changes in lung structure could be observed. After 48 hours the interstitial space was enlarged by accumulation of fluid and early destructive changes of the capillary endothelial lining were found. After 72 hours the widened interstitial space contained numerous leucocytes, thrombocytes and other cells; fibrin strands were numerous. There was marked destruction of the pulmonary capillaries. At this stage, 65% of all alveoli were filled with an exudate containing leucocytes, erythrocytes, macrophages and fibrin strands. There was a decrease in capillary blood volume and of endothelial surface after 72 hours. The thickness of the air-blood barrier was increased after 48 and doubled after 72 hours. The barrier thickening was mainly due to increase of the interstitial space; terminally, the epithelium was also thickened, although the endothelium became thinner, on the average, due to destruction. As a result of these alterations there was a marked fall in estimated gas exchange capacity of the air-blood tissue barrier.

I. INTRODUCTION

The purpose of this study was to establish the time-sequence of changes occurring in the lung as a result of continued breathing of pure oxygen at atmospheric pressure. As the primary site of contact of O_2-molecules with tissue the lung is particularly well suited for a study of the uncomplicated damaging effects of oxygen at elevated partial pressures, which occur in a relatively short time. Because of the requirements of breathing 100 % oxygen for life support in aviation and space travel, a systematic evaluation of these effects appeared urgently needed.

At the outset of our study the following findings had been obtained by various investigators on humans and on laboratory animals (for a detailed review see ref.1).

Among the clinical symptoms of oxygen poisoning severe dyspnoe prevailed. This correlates to the chief functional findings of a reduction of vital capacity (2, 3, 4, 5, 6, 7)* and of diffusing capacity of the lung (7, 8), as well as to an observed decrease of the hemoglobin content of the blood (3, 9, 10) apparently associated with hemolysis (11, 12). Recent investigations have also revealed a change in the surface active properties of lung extracts in dogs (13).

A large number of pathological findings were obtained on oxygen poisoned lungs; they can be grouped into three categories:
a. Observed changes in airway structure consisted mainly in atelectasis (9, 12, 14, 15) and in an accumulation of exudate in the alveoli, which contained numerous red cells, leucocytes and macrophages (2, 5, 14, 16, 17, 18, 19, 20). It was partly fibrinous and occasionally appeared to form "membranes" on the alveolar walls (14).
b. Among vascular changes hyperemia was observed by numerous investigators (1). A massing of thrombocytes in lung capillaries, as well as a tendency of blood cells to agglomerate was also found. (14). Pratt has suggested that a proliferation of capillaries may occur (21).
c. In the lung tissue a peribronchial and perivascular edema was observed with the light microscope (14, 19). Electron microscope studies revealed a thickening of the alveolocapillary tissue barrier due to accumulation of fluid in interstitium and cells (14). In addition, changes in organelles of alveolar epithelial cells appeared to occur, such as swelling of mitochondria (22) and an increase in the number of "lamellated bodies" (14).

In appraising all these studies we note that the pathological investigations were phenomenological in nature; that is, they

---

* Such numbers refer to Reference section.

were restricted to a thorough description of the different pathological observations made on tissue preparations. For this purpose these studies were done on "terminal" stages of "tolerable" oxygen exposure where the picture is striking. A systematic study of the time sequence of the development of pulmonary damage due to breathing pure oxygen was therefore indicated. Furthermore, the pathological studies quoted lacked quantitative information on extent and severity of the observed damages. In order to define the time sequence of events, and to indicate the influence that observed changes may have on the functional performance of the lung as a gas exchange apparatus, morphometric methods (23, 24) were employed in the present study which availed itself of gross observation, light microscopy and electron microscopy.

II. EXPERIMENTAL DESIGN

The first experimental step involved the exposure of rats to an atmosphere of pure oxygen under controlled conditions. This was done in collaboration with the 657oth Aeromedical Research Laboratories at Wright-Patterson Air Force Base, Ohio, in one of their environmental chambers. After removal of the anesthetized animals from the chamber the lungs were immediately processed according to the scheme given below. The specimens were further evaluated in the Laboratory for Electron Microscopy of the Department of Anatomy, University of Zürich.

A. Specifications of the environmental chamber used

1) Chamber description (see Fig.1)

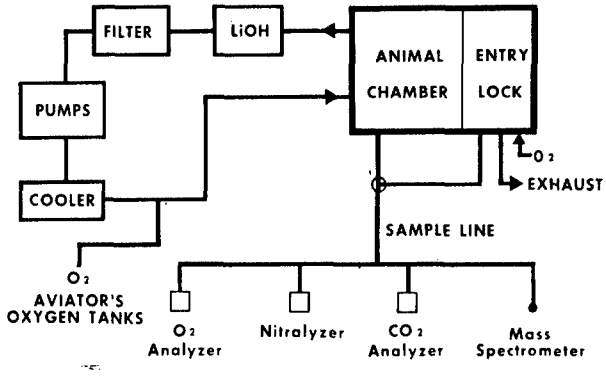

Fig.1: Diagram of environmental system.

The chamber at 657o th AMRL was cylindrical in shape, made of aluminium with a jacket of spun fibre glass aircraft insulating material. The volume of the main cell (experimental department) was 17o ft^3.

The chamber atmosphere was recirculated through a closed circuit pump system with a flow rate of about 15 ft^3/min at one atmosphere. The carbon dioxide concentration was maintained below o.1 % by

absorption in lithium hydroxide cannisters. Odors were removed by activated charcoal in the cannisters. Temperature and humidity were controlled by the cooler system. The oxygen source consisted of cylinders of gaseous aviators breathing oxygen, with minimum 99.5 % concentration.

Sampling of the chamber atmosphere through the various analyzers was continuous, with the exception of the mass spectrometer analysies (see below).

All entries to the chamber were done through the entry lock in which atmospheric composition and pressure could be matched to that inside the main cell, thus avoiding contamination of the test atmosphere with nitrogen.

2) Controls concerning toxic contaminants.

In a special study by the group at 657o th AMRL (7), using a second but very similar chamber model, the chamber atmosphere was analysed with respect to possible contaminants while operating under experimental conditions. A mass spectrometer analysis of room air and the chamber atmosphere showed them to be essentially the same with respect to trace gases. Furthermore, analysies for oxidants were made by the neutral buffered potassium jodide technique (25) and for lithium with emission spectrography, because these substances are specifically toxic to the lung in concentrations smaller than might be detected by the mass spectrometer. Total oxidants were present in amounts of o.1 ppm or less by volume. There was no ozone detectable by smell which probably means that ozone was not present in concentrations greater than o.o4 ppm by volume (26). Nor was there any means of ozone production by either ultraviolet light or spark in this system. Lithium was present in concentrations of only 1 microgram or less per m^3 of chamber atmosphere.

Since the same pumps were used in both chamber systems (chamber for the control of toxic contaminants and chamber for the experiments presented in this paper) we can conclude that there were no toxic contaminants present in sufficient concentrations to produce by themselves the effects observed after experimental exposure of the animals to 98.5 % O_2 at one atmosphere. Thus, the respective tests done on the aluminum chamber used for the experiments presented here, could be reduced to periodic checks by the mass spectrometer analysis of the chamber atmosphere. These have never shown the presence of any mass not also present in ordinary room air.

However, the possibility cannot be absolutely ruled out that in an atmosphere of 98.5 % oxygen minor concentrations of oxi-

dants or lithium may act synergistically with oxygen and play a role in the pathogenesis of the changes in pulmonary functions seen. The probability of such an interference can, however, be estimated as very minute.

B. O_2-Exposure Experiments.

1) Exposure of rats to 98.5 % O_2 at 765 mmHg.

Of 98 male Sprague-Dawley rats born on the same day, 73 were simultaneously exposed to 98.5 % O_2 at one atmosphere ambient pressure. They were removed from the chamber in groups according to the following schedule:

Experimental group:	B 1	after 6 hours in chamber
	B 2	" 24 " " "
	B 3	" 48 " " "
	B 4	" 72 " " "

A group of 14 animals, kept in room air under otherwise identical conditions, were sacrificed as controls (CB) and processed in the same way as the test animals. A random sample of 11 rats had been sacrificed before the experiment as gross quality control (QB). Table I indicates that the homogeneity of the material used in this study was satisfactory.

Table I: Characteristics of animals used in study:

Group	Number of animals	age at sacrifice days	average body weight gm	S.D. gm	Murine pneumonia number of animals	% incidence
Q B	11	43	-	-	o	o
C B	14	44	122.6	2.5	1	7
B 1	18	47	116.o	o.7	1 (1) *	11
B 2	17	48	119.o	3.5	1 (1) *	12
B 3	17	49	123.o	4.3	o	o
B 4	24	5o	1o2.4	6.o	o	o

* (1) - Questionable pneumonia.

The incidence of murine pneumonia was slight. For the quantitative studies reported here only lungs were used which were free of any signs of this disease.

For these experiments at one atmosphere, the inside of the environmental chamber was pressurized 25 mmHg higher than outside ambient pressure (740 mmHg), thus ensuring that any possible leaks in the system were outboard. The main physical characteristics of the chamber atmosphere can be given as follows:

Total ambient pressure:	740 + 25 mmHg
Oxygen concentration:	98.5 % ± 1 % *
Carbon dioxide concentration:	below 0.1 %
Relative humidity:	46 ± 1 % *
Temperature:	74 ± 2° F *

* The ± values represent one standard deviation.

2) Exposure of rats to 98.5 % O_2 at 258 mmHg.

In the course of our work at 6570th AMRL a second experiment was performed, exposing a similar group of rats to 98.5 % O_2 at 1/3 atmosphere ambient pressure. Their lungs were processed in the same fashion. The results obtained on this group will be reported later.

C. Preparation of Lungs

1) Fixation of lungs.

At the end of each experimental series, the animals were deeply anesthetized by intraperitoneal injection of a body-weight-conform amount of pentobarbital, then brought out of the chamber, weighed, labeled, and immediately processed in the following way:
a. Exposure of chest and trachea, tracheotomy.
b. Puncture of chest and instillation of fixative (cold 2.5 % glutaraldehyde in 0.03 M K-phosphate buffer, pH 7.4)* through a fine polyethylene catheter inserted into the trachea and fixed by ligature. The instillation fluid was prepared in burettes; at the start of flow the hydrostatic pressure was consistently standardized to 20 cm H_2O. Flow of fixative into the air spaces was allowed until equilibration. Under these conditions, the

* In a preliminary study, the isotonicity of the solutions used was thoroughly tested on different rat tissues.

lungs were all inflated to their maximum extensibility in the chest cavity.
c. Ligature of the trachea with the previously placed thread while withdrawing the cannula.
d. Removal of lung and heart and immediate submersion in the same fixative solution for 2 hours.
e. Dissection of heart and mediastinal tissue from the lungs
f. Measurement of the lung volume by fluid displacement **, using the fixative as immersion medium.

At the same time and under the same conditions, a few randomly sampled lungs were fixed as technical controls with 1 % OsO_4 in o.1 M K-phosphate buffer.

After fixation for two hours, the lungs were carefully sliced from top to bottom into alternately thick (3-5 mm) and thin (1mm) slices. From this point on, two different standardized processing sequences were used:

2) Preparation of specimens for light microscopy:

The thick lung slices were placed into fixative in labeled snap caps and carried to Zürich, where they were further processed according to the following schedule:
a. washing in 5 changes of o.11 M K-phosphate buffer for 5 days.
b. dehydration in graded ethanol.
c. double-embedding in celloidin-paraffin.

From these blocks, histologic sections of ca. 8μ were cut on a sliding microtome and stained with the standard procedures for Hematoxylin-Eosin, PAS, Goldner, and Elastin-van Gieson stains.

3) Preparation of specimens for electron microscopy.

The thin slices of each lung were carefully cut into some 2oo small cubes of approximately 2 to 3 mm^3, and processed according to the following schedule***:
a. washing in 3 changes of o.11 M K-phosphate buffer for 2 hours.
b. postfixation in 1 % OsO_4 buffered to pH 7.4 on ice for 9o min.
c. dehydration in graded ethanol.
d. embedding in Epon 812 according to the method of Luft (27).

Sectioning of the Epon embedded specimens was done on a LKB Ultrotome and on a Porter-Blum Ultramicrotome using a DuPont diamond knife. Section thickness was about looo Å; for special

---

** A special test proved the accuracy of this method to be very satisfactory.
*** Processing took place at 6570th AMRL on the day of removal of the animals from the chamber.

purposes thinner sections (500-600 Å) were also used. The sections were picked up on 150 mesh copper grids fitted with a thin Formvar film reinforced by carbon. They were contrasted by the lead citrate method of Reynolds (28).

4) Preparation of specimens for histochemical studies.

Some lungs of each experimental group were quick-frozen without prior fixation. The trachea of the anesthetized animal was tied with a string to avoid collapse of the lung. The chest organs were rapidly excised in toto and immersed in isopentane chilled to -140°C by liquid N_2. The frozen lungs were stored in liquid N_2 and used for histochemical enzyme studies, the results of which will be reported later.

III. MORPHOMETRIC METHODS.

A. Sampling procedure.

The total material resulting from the exposure experiments consisted of the lungs of all animals belonging to the respective experimental groups. Only a minute sample could eventually be investigated. Particular attention had thus to be given to a proper multiple stage sampling procedure.

1) Sampling of animals.

Upon removal from the chamber all animals were consecutively numbered. The lungs were fixed as outlined above. Those lungs which showed typical signs of murine pneumonia on gross examination or accidental technical artifacts were eliminated and processed separately. The remaining lungs were renumbered consecutively. Eventually the first 5 lungs of each group were chosen for the quantitative studies reported here.

2) Sampling of specimens for light microscopy.

All thick slices of the lungs (see above) were processed to celloidin-paraffin-blocks. For each animal these blocks were aligned in order of size, and a systematic sample of five blocks (every third block) was drawn; these blocks were sectioned and used for quantitative analysis in the light microscope. On the sections, the fields to be evaluated were systematically sampled by displacement of the slide by exactly 1 mm by means of a calibrated microscope stage.

3) Sampling of specimens for electron microscopy.

The thin slices of all suitable lungs (see above) were cut into

some 2oo small cubes of 2-3 mm^3 volume. In the course of further processing they became thoroughly mixed, so that a random sample of ten blocks could be picked for each animal; they were again consecutively numbered. The smallness of the block and their deep black colour due to OsO_4-fixation made a biased sampling impossible. The remaining blocks were bulk-embedded as reserves.

For each of the five investigated animals per group the first five blocks were sectioned; the sections were mounted on copper grids. The position of the section was delineated on a master sheet on which each square of the copper grid was assigned a number. By means of a random number table six fields were selected in the electron microscope and electron micrographed at standard magnification on 35 mm film, irrespective of the content. Fields with technical defects were not recorded but replaced. All recorded fields were used for study. Details of this sampling method were described earlier (23, 29). By this procedure, 3o electronmicrographs were quantitatively evaluated for each animal, making 15o for each experimental group and for the controls. This gave a total of 75o random electronmicrographs, based on 125 ultrathin sections.

B. Stereologic principles employed.

All stereologic methods of measurement employed in this study have been reported earlier in detail (23, 29, 3o) so that only the essential points shall be stated here.

1) Volumetric analysis.

The volume relationship between different components was estimated by differential point counting (31). A lattice of P regularly spaced points is randomly placed on a section of the material to be studied. A number P_A of these points will be lying on sections of the component A.

The ratio

$$\frac{P_A}{P} = V_{VA} = \frac{V_A}{V} \qquad (1)$$

will be an estimate of the relative volume occupied by the component A, V_A being its absolute volume and V the total containing volume.

2) Surface area measurement.

If a linear probe of length L is randomly placed on a section of tissue the number of intersections N_A of this line with the

surface of a component A is proportional to its surface area S_A (32). If the surface is contained in a volume V

$$S_A = \frac{2 \cdot V \cdot N_A}{L} \qquad (2)$$

It is not necessary that the linear probe be very long; we can also distribute Q short lines of length z on the section whereby $L = Q \cdot z$.

3) Surface-to-volume ratio estimation.

If a component A, contained in a volume V, has an over-all surface S_A and a total volume V_A, then some information on its geometric properties can be derived from its surface-to-volume ratio. From eq. (1) and eq. (2) we obtain

$$\frac{S_A}{V_A} = \frac{2V \cdot N_A}{L} \cdot \frac{P}{P_A \cdot V}$$

$$= \frac{2P \cdot N_A}{L \cdot P_A} \qquad (3)$$

Dividing the linear probe of length L into Q short lines of equal length z, and using the 2Q endpoints of these lines as the P test points for volumetric analysis, eq. (3) becomes

$$\frac{S_A}{V_A} = \frac{4 \cdot N_A}{z \cdot P_A} \qquad (4)$$

In this principle, which goes back to Chalkley et al. (33), the number of test lines used does not enter into the relation anymore.

4) Estimation of arithmetic mean thickness of a tissue sheet (air-blood-barrier).

The average thickness $\bar{\tau}$ of a double-surfaced tissue sheet can be defined as the average tissue volume per surface area (29); $\bar{\tau}$ can thus be obtained by inversion of equation (4) to

$$\bar{\tau} = \frac{z \cdot P_T}{2 \cdot N_S} \qquad (5)$$

where P_T is the number of end-points of the test lines of length z falling onto tissue and N_S is the number of intersections of the test lines with both surfaces. The numerical coefficient is 2 instead of 4 because both surfaces contribute to N_S (compare 29).

5) Estimation of harmonic mean thickness of barrier.

In appraising the properties of the air-blood barrier as a diffusion resistance for gases an estimate of its harmonic mean thickness has to be obtained (23, 24, 29), which is defined as

$$\tau_h = \frac{\Sigma f_i}{\Sigma f_i \cdot \tau_i^{-1}}$$

where f_i is the frequency of a thickness τ_i. According to a principle developed in an earlier report (29) τ_h can be estimated from the harmonic mean ℓ_h of the random intercept length ℓ, measured along randomly placed linear probes of infinite length from entry to exit point, by the formula

$$\tau_h = \frac{2}{3} \cdot \ell_h = \frac{2}{3} \cdot \frac{N}{\sum_{i=1}^{N} \ell_i^{-1}} \qquad (6)$$

6) Counts.

Counts of red cells and nuclei were carried out by counting the number n_A of their transsections appearing within the test area of given size ($5.4 \cdot 10^{-4}$ cm^2) on electron micrographed sections. The number N_A of these structures contained in the unit volume of lung tissue could have been calculated by the formula of Weibel and Gomez (23, 34) as

$$N_A = \frac{n_A^{3/2}}{\beta_A \cdot V_{VA}^{\frac{1}{2}}} \qquad (7)$$

where β_A is a shape coefficient. However, we have abstained from this calculation, since we were only interested in comparing different experimental groups; and this could well be done by comparing the numbers of transsections.

C. Practical application.

1) Stereologic analysis of sections in light microscope.

The light microscope could be used to estimate on celloidin-paraffin sections the amount of damage caused to alveoli in more

advanced stages of oxygen poisoning. This was done by volumetric analysis,as described above,using the Zeiss Integrating Eyepiece I, as proposed by Hennig (31), together with a 2o x objective on a WILD M-2o Microscope.

2) Stereologic analysis of electronmicrographs.

Random fields of ultrathin lung sections were micrographed at constant magnification on a Philips EM 2oo electron microscope. The recording material was 35 mm film which could accomodate all 3o micrographs obtained from the 5 sections of one test animal. In addition a calibration standard was also recorded on each strip. These negatives were contact printed on positive film. The positives thus obtained could be passed, frame by frame, through a small table projector unit especially constructed for this purpose. A mirror reflected the image on a screen made of frosted acetate foil between two glass plates. This screen was fitted with a suitable lattice of points and lines with which volume ratios, surface areas etc. could be estimated by simple counting, as outlined above.

For the measurement of intercept lengths of long random probes with the barrier, this lattice was replaced by a system of parallel lines, along which the intercept lengths ℓ were measured with a logarithmic scale. This scale was chosen to minimize the error of measurement in the short values of ℓ, which influence the harmonic mean most severely.

3) Differential counter.

To facilitate and rationalize the recording of the large number of counts - in this experimental series alone,13o'ooo points had to be differentiated, plus some 2o'ooo intersections with surfaces - a differential counter was constructed of small electrical units. Through a set of lo microswitches the investigator could "feed the location of a point" into a particular unit, where this information was added to previously entered information.

D. Statistical analysis of data.

For the present report a simple and rapid method of statistical evaluation has been used. Each quantitative information sought was calculated for each test animal individually, each animal being taken as a sample unit. (Variation among the subsamples such as sections or fields is presently not considered). The parameter under consideration of animal j in group i being y_{ij} the following group information was calculated, with 5 animals per group:

$$\bar{y}_i = \frac{\sum_{j=1}^{5} y_{ij}}{5} \qquad (8)$$

$$S.D._i = \frac{\sum_{j=1}^{5} (y_{ij} - \bar{y}_i)^2}{4}$$

$$= \frac{\Sigma\, y_{ij}^2 - \bar{y}_i \cdot \Sigma y_{ij}}{4} \qquad (9)$$

$$S.E.(\bar{y}_i) = \frac{S.D._i}{\sqrt{5}} \qquad (10)$$

All ± values indicated in the tables are one S.E. (unless otherwise indicated). In the graphs the two brackets above and below the average point enclose two S.E.

The comparison of the different test groups was done by Student's t-test, using the following formulas, S_1^2 and S_2^2 being the variances of the two estimates:

$$S_d = \sqrt{\frac{N_1 \cdot S_1^2 + N_2 \cdot S_2^2}{N_1 + N_2}} \quad , N_1 = N_2 = 5 \qquad (11)$$

$$t = \frac{|\bar{y}_1 - \bar{y}_2|}{S_d} \cdot \sqrt{\frac{N_1 \cdot N_2}{N_1 + N_2}} \qquad (12)$$

The degree of freedom being $N_1 + N_2 - 2 = 8$

we find the following error probabilities:

$t > 1.86$	$P < 0.1$
$t > 2.31$	$P < 0.05$
$t > 3.36$	$P < 0.01$

It is realized that this test is relatively crude and that more information could have been ascertained by applying a multiple variance analysis. However, this time-consuming test is postponed until the results obtained on the second O_2-exposure experiment at 1/3 atmosphere pressure are complete. The two experimental series will then be thoroughly tested and compared, applying an elaborate multiple variance analysis. It can be said, however, that this extended testing will reveal at least as much information as is presented here. Some points which only appear suggestive today may be proven to be factual.

IV. RESULTS

A. Description of damages observed.

1) Gross findings at autopsy at end of exposure experiments.

All animals showing typical gross signs of (endemic) murine pneumonia (see table) were eliminated from the test series because of pathological complications unrelated to - or only partially aggravated by - oxygen poisoning.

In each of the groups B1 and B2 one animal which showed signs of focal consolidation suspicious of pneumonia was also eliminated from the series for quantitative study, but prepared for light microscopic investigation. The lungs of all other animals of these two groups appeared grossly normal.

At transfer from the high O_2 atmosphere to room air most animals of the B3 group showed signs of dyspnea of varying severity. The pleural cavity contained in all cases some exudate, mostly yellowish but occasionally slightly hemorrhagic. The lung surface was mottled with dark and light patches of a few millimeters diameter.

The animals of the B4 group were severely dyspnoic when brought to room air; they were gasping and rapidly became cyanotic. Some animals died within a few minutes. Upon opening the chest large amounts of partly hemorrhagic pleural exudate were found in all cases. The mottling of the lung surface was very striking.

An interesting finding relates to the volume of fixative that could flow into the lungs from the burettes. In groups CB, B1 and B2 this amounted to 6 ml on the average. In B3 it was reduced to 5 ml, and in B4 even to 2.6 ml. This may partially have been due to the presence of pleural exudate, but partially also to pulmonary edema as described below.

In groups B3 and B4 the livers and spleens showed increasing signs of congestion, indicating right heart failure.

2) Light microscopic findings.

In Figs. 2 and 3 a low power micrograph of a section of a normal control lung CB is confronted with a corresponding section from a B4 lung (72 hours in 98.5 % O_2). In the normal lung the very fine regular pattern of airspaces is easily recognized. In Fig. 3 this pattern appears preserved in a few areas but is obliterated in other regions. This is due to an accumulation of exudate in alveoli and air ducts, as can be seen more clearly in Figs. 4 and 5 which also show the patchy distribution of exudate. A certain portion of the lung appears more or less normal at this level of resolution. A quantitative appraisal of the relation between "normal" and pathological alveoli will be reported below.

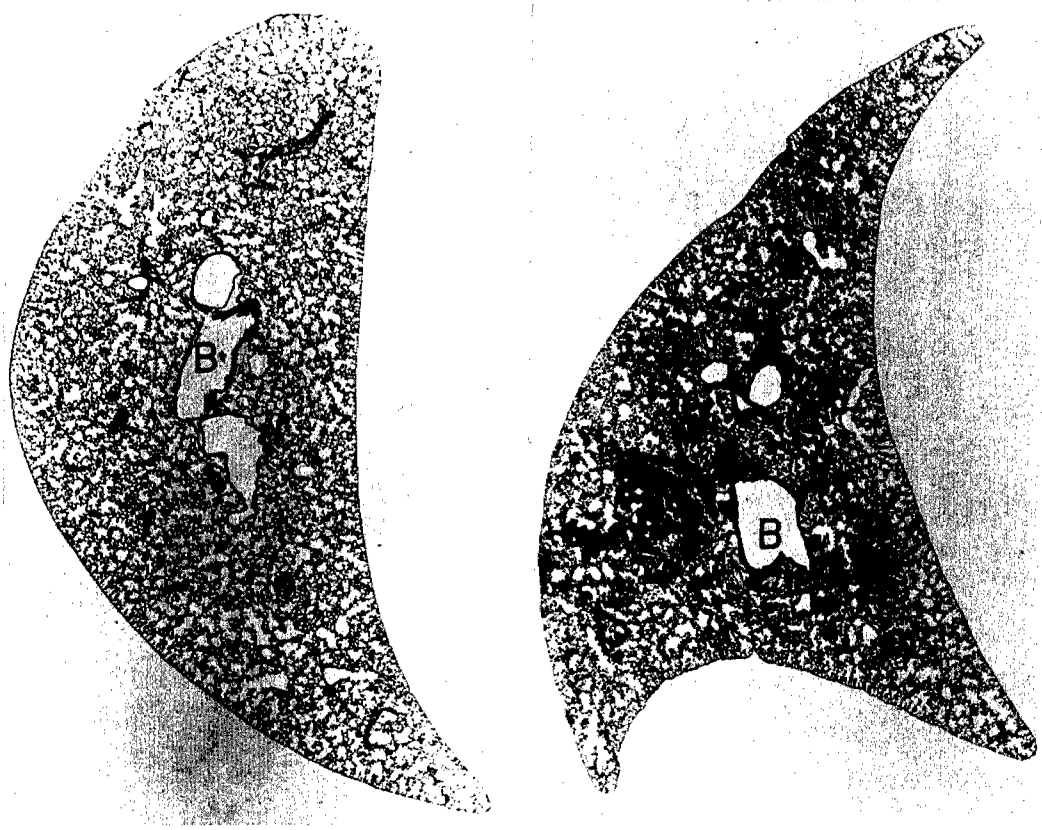

Fig. 2 Control lung CB. B = bronchus. Goldner stain. x 11.

Fig. 3 B4 lung. Observe patchy accumulation of exudate in airways, as well as perivascular edema. B = bronchus. Goldner stain. x 11.

The alveolar exudate appears to consist of three components: Most of the affected alveoli are filled with a structureless fluid assuming a green colour in Goldner's trichrome stain, which indicates its protein content (Fig. 5). Within this exudate an extraordinarily high number of alveolar macrophages is found (Figs. 5 and 6), while in other regions masses of fibrillar material are found (Fig. 7) which consists of fibrin, as will be shown below.

The interalveolar septa of B4 lungs appear thickened with an increased number of constituant cells, while the blood capillaries seem somewhat less conspicuous than in normal lungs. In contrast to these striking findings in the terminal test group B4, the lungs of the rats of groups B1, B2 and B3 showed not much of a pathological appearance. In the groups B1 and B2, no alveolar exudate was observed. There was some indication of an irregularity in the filling of capillaries with blood; however, it could not be excluded that this subjective interpretation could be related to a variation in seetion thickness. In the B3 lungs there appeared an indication of beginning formation of alveolar exudate as seen in the terminal group. The number of alveolar macrophages was somewhat increased.

Figs. 3 and 4 show that the normally narrow connective tissue space enveloping the larger blood vessels is strikingly edematous in the B4 lungs. This perivascular edema can also be observed in the B3 lungs, but not in the earlier stages.

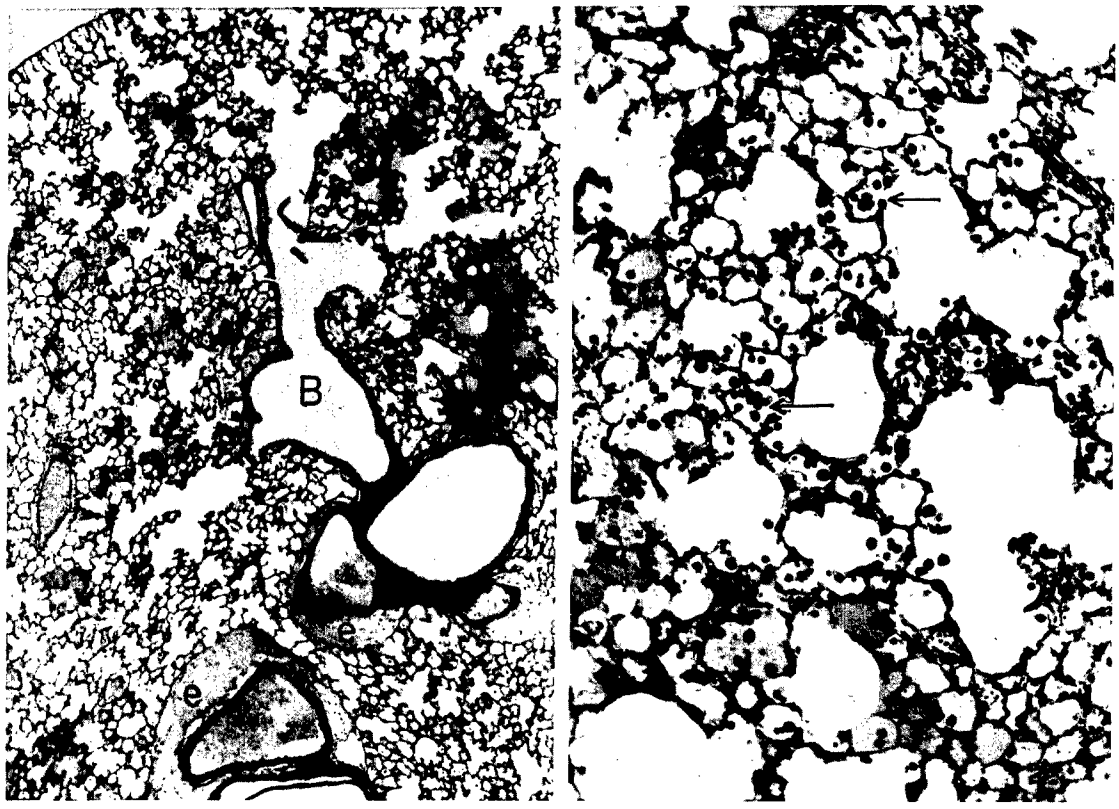

Fig. 4 B4 lung. Patchy accumulation of exudate. Perivascular edema (e) near bronchus B. Goldner stain. x 4o.

Fig. 5 B4 lung. Exudate and numerous macrophages (arrows) in alveoli. Goldner stain. x 3oo.

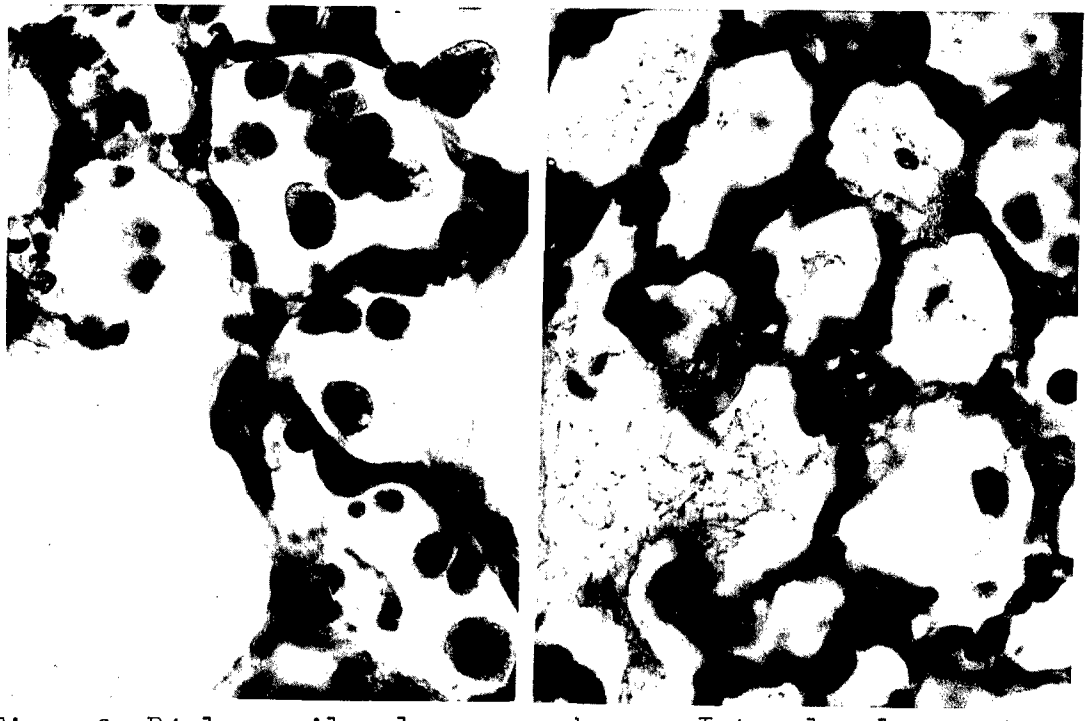

Fig. 6 B4 lung. Alveolar macrophages. Interalveolar septa thickened. Goldner stain. x 75o.

Fig. 7 B4 lung. Fibrin threads in alveoli with exudate. Interalveolar septa thickened. Goldner stain. x 75o.

It has become clear from the preceding description that only a limited amount of substantial information can be drawn from standard histological preparations. Their main defect is the section thickness which is of the same order of magnitude as the interalveolar septa and the capillaries. We have therefore extended these studies by observing thinner sections (o.5 - 1 μ) in a phase contrast microscope. As illustrated by Figs. 8 - 11, this method brings a con-

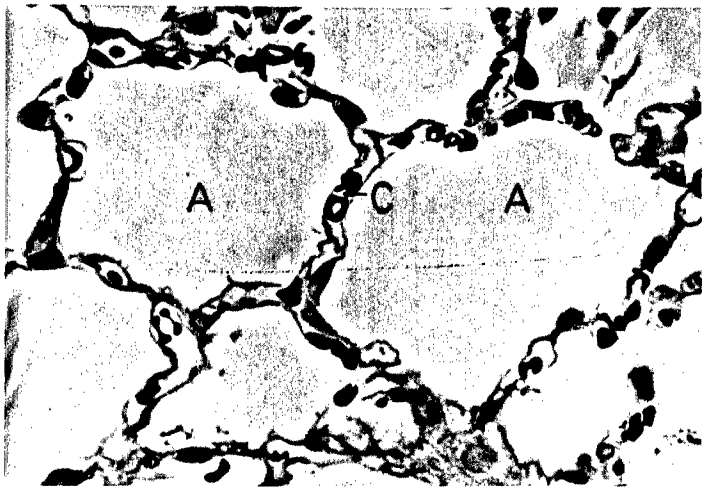

Fig. 8 Control lung CB. Phase contrast micrograph of thin section. Note red cells in capillaries and delicate air-blood barrier. x 6oo.

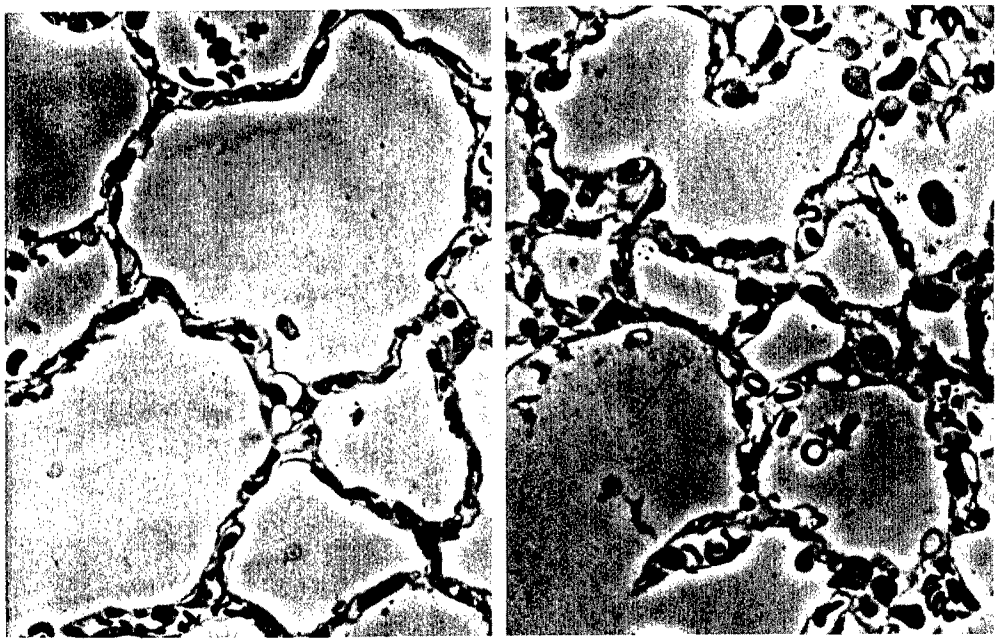

Fig. 9 B3 lung. Phase contrast micrograph of thin section. Relatively normal portion. x 6oo.

Fig. 1o B3 lung. Phase contrast micrograph of thin section. Thickening of interalveolar septa and beginning formation of alveolar exudate (arrows).

siderable gain in resolution, and still allows surveys of larger fields. It thus forms an excellent intermediary to electron microscopy.

In the normal lung the alveolo-capillary membrane separating air and blood can be clearly distinguished (Fig. 8). Fig. 9 shows that similar areas with normal appearance occur in B3 lungs. In other regions of these lungs (Fig. 10) the alveolo-capillary tissue layer appears thickened and some exudate has formed on the alveolar wall. Fig. 11 shows a region of a B4 lung in which the alveolo-capillary tissue is greatly thickened; the number of cells is increased. The alveolar exudate described with respect to Figs. 3 - 7 is also seen. Corresponding sections of lungs of the B1 and B2 group revealed no pathological findings.

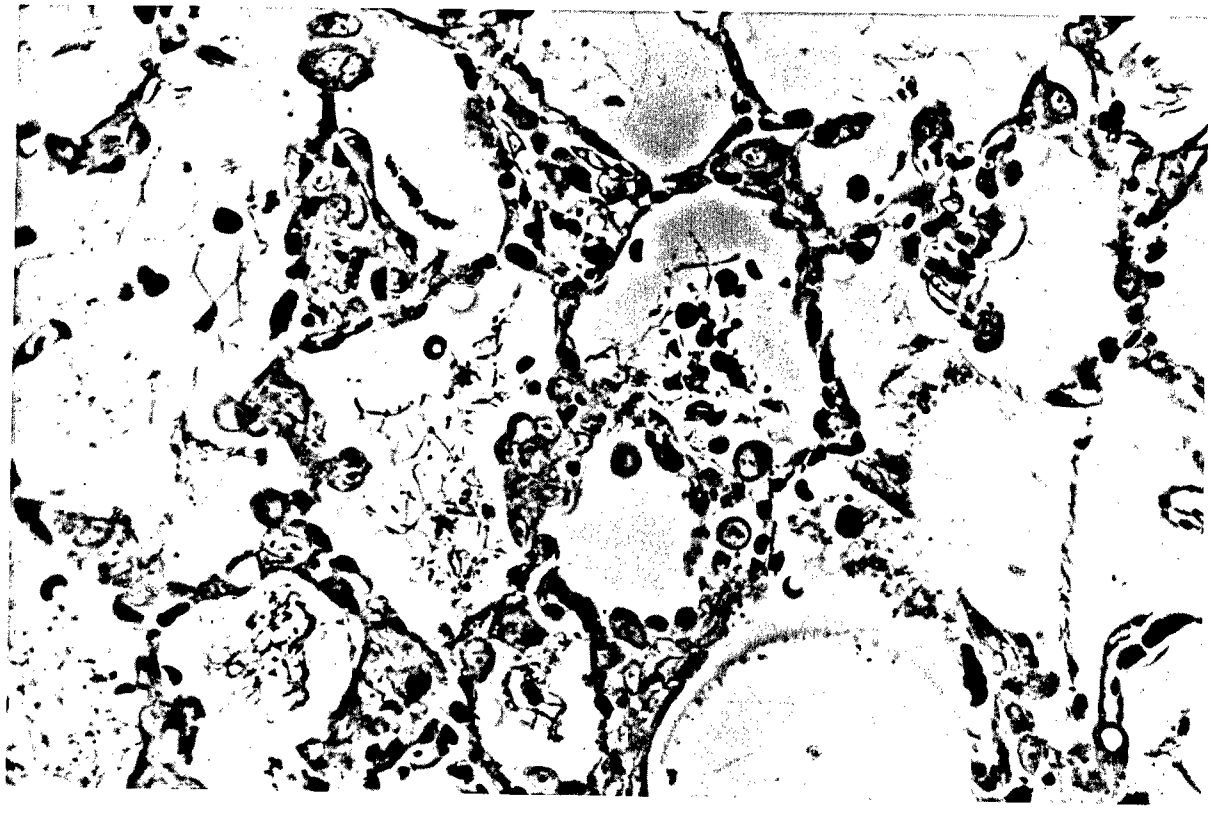

Fig. 11 B4 lung. Phase contrast micrograph of thin section. Severe thickening of interalveolar septa with increased number of cells and obliteration of capillaries. Alveoli filled with exudate containing red cells, cell debris and fibrin threads.

3) Electron microscopic findings

Fig. 12 illustrates the relevant features of the fine structure of the normal rat lung (CB) at the alveolo-capillary level. The capillaries are lined by a thin endothelial cell layer; the alveoli are lined by an epithelial layer which, for the most part, is equally thin. Some large cells containing the characteristic "lamellated bodies" are incorporated into this epithelium (Fig. 12b). It is particularly relevant to note that the interstitium which separates endothelium and epithelium is mostly very narrow. In some regions between capillaries the interstitium is wider and contains fibroblasts, collagenous and elastic connective tissue fibers (Fig. 12a and b). It should be emphasized, however, that the fluid ground substance between these formed elements occupies only an extremly narrow space, as seen in Fig. 12b.

In Fig. 13 two corresponding fields from a section of a B3 lung are reproduced. The striking enlargement of the interstitial space is quite evident. It is due to an accumulation of fluid in the ground substance space, which caused a wide separation of the formed interstitial elements, as well as of endothelium and epithelium. An extreme instance of this interstitial edema is shown in Fig. 14; the nature of the very fine dark granules in the edematous fluid is not clear. In more severely damaged regions of B3 lungs we observe an infiltration of the tissue with leucocytes and a beginning destruction of endothelial cells (Fig. 15). Though such areas are relatively scarce they are indicative of the third day of exposure to pure oxygen.

Key to symbols on electron micrographs

A	Alveolus	EP	Alveolar epithelial cell
ACB	Alveolo-capillary barrier	FB	Fibroblast
BM	Basement membrane	FN	Fibrin
C	Capillary	LB	Lamellated body
CF	Collagen fibrils	LC	Leucocyte
EC	Erythrocyte	M	Mitochondrion
ED	Interstitial edema	MF	Myelin figure
EL	Elastic fibers	N	Nucleus
EN	Capillary endothelial cell	T	Thrombocyte

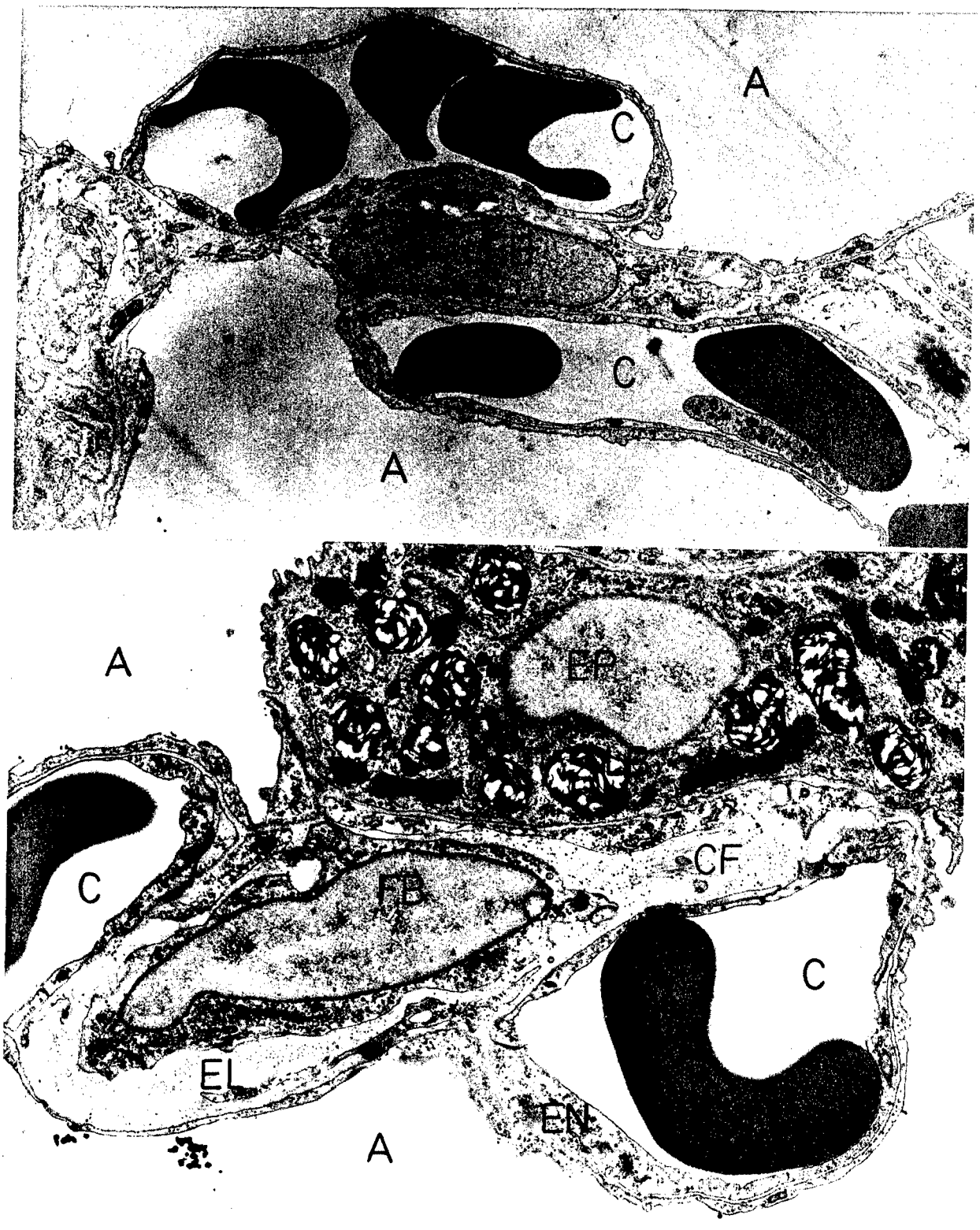

Fig. 12 Electron micrographs of Control lung CB.
a) low power view of interalveolar septum. Note delicate alveolo-capillary barrier and narrow interstitial space. x 6'3oo.
b) Fibroblast and connective tissue fibers in narrow interstitial space between capillaries. Epithelial cell with lamellated bodies. x lo'5oo.

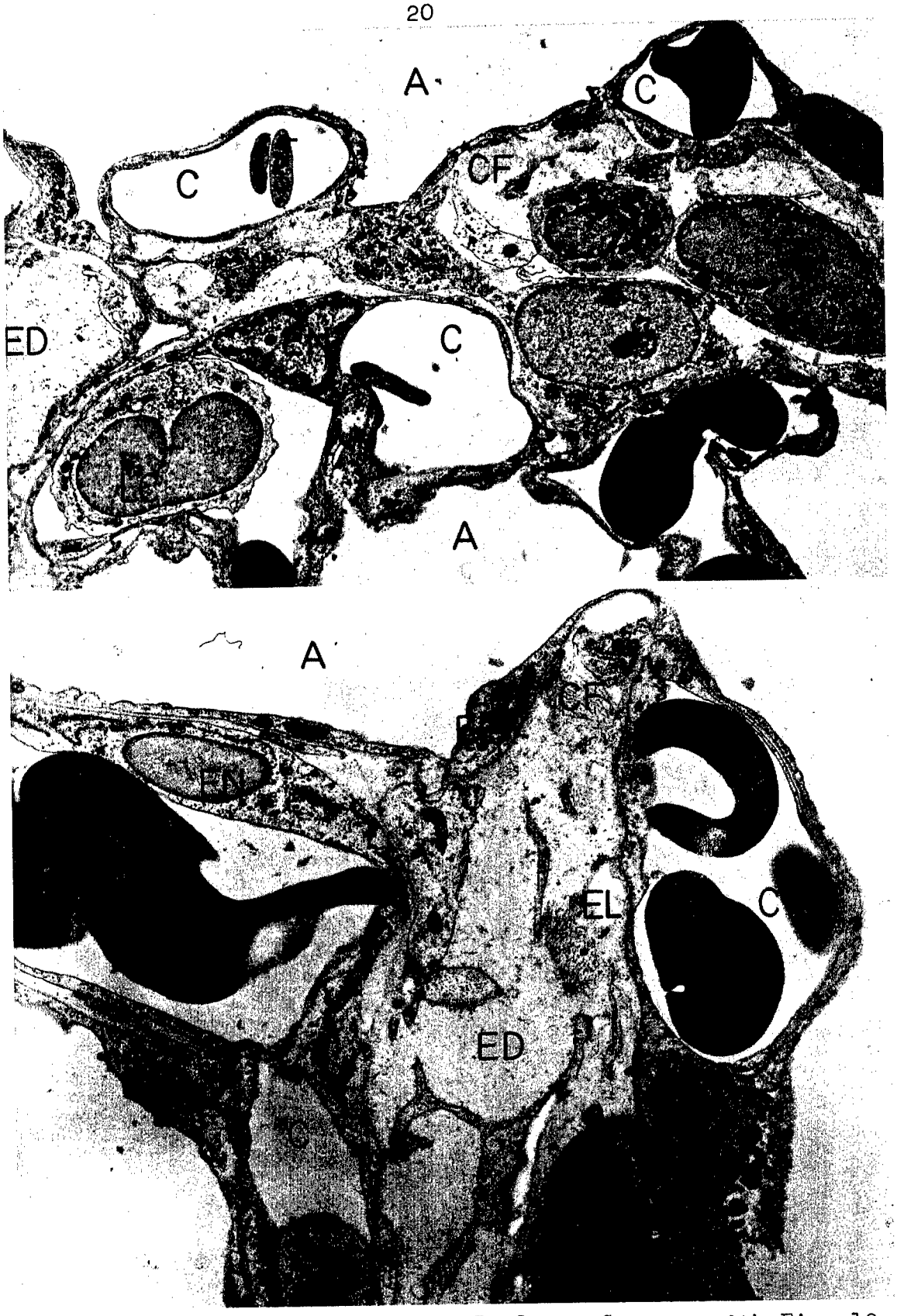

Fig. 13 Electron micrographs of B3 lung. Compare with Fig. 12.
a) low power view of interalveolar septum. Widened interstitial space with edema and increased number of interstitial cells. x 4'7oo.
b) Widening of interstitial space by edema. Note separation of capillaries and fibers. x lo'5oo.

Figs. 16 - 21 illustrate the damage established at 72 hours in the B4 group. Comparing the low power electron micrograph of Fig. 16 with Figs. 12a and 13a it can be realized how far away from normal the situation at the alveolo-capillary level is. Capillaries are hardly recognized, except for their content of highly distorted and partially fragmented erythrocytes.Fig. 17 illustrates the destruction of endothelial cells characteristic of this stage. Often, red cells are seen to be in immediate contact with the endothelial basement membrane (Fig. 18), indicating the complete disappearance of the endothelial lining in such regions. In the interstitium the striking edema observed in the B3 lungs has disappeared. It is replaced by numerous interstitial cells, partly identifiable as

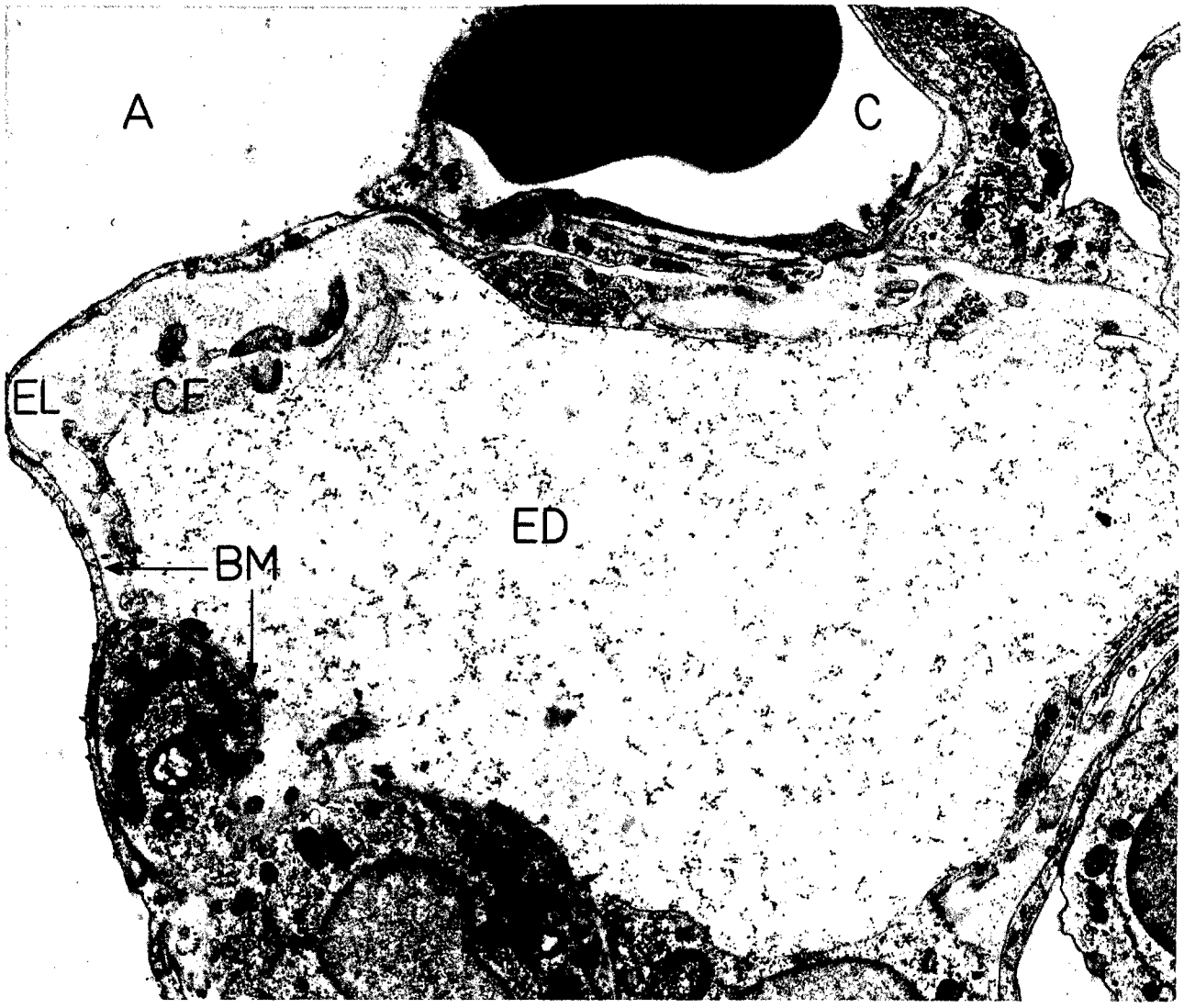

Fig. 14 Electron micrograph of B3 lung. Massive accumulation of edema fluid in interstitial space. x lo'5oo.

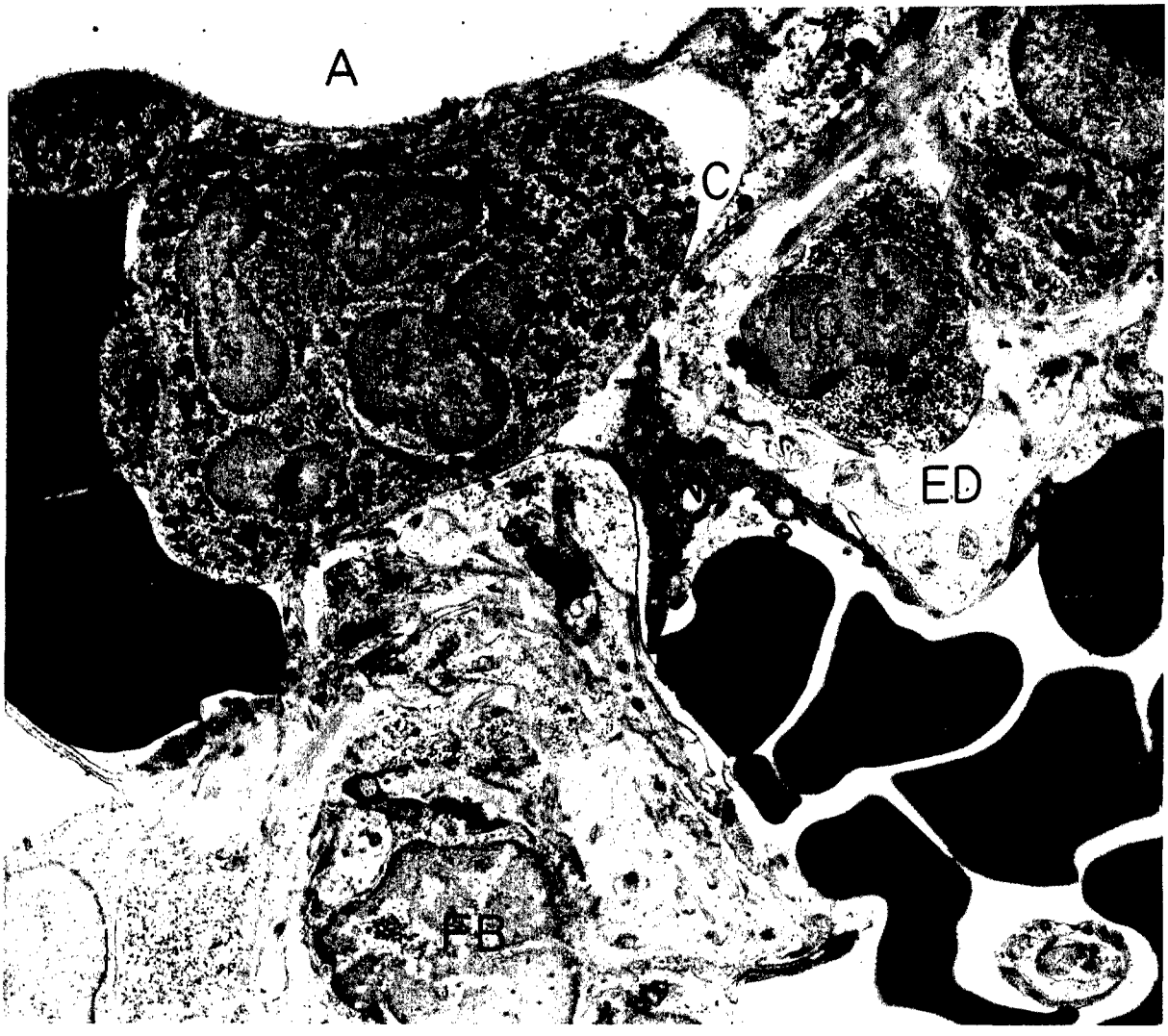

Fig. 15 Electron micrograph of B3 lung. Heavily damaged region. Intravascular and interstitial leucocytes with phagocytosed material. Partial destruction of capillary endothelium (EN'). Interstitial fibrin formation. x 7'7oo.

Fig. 16 Low power electron micrograph of interalveolar septum of B4 lung. Compare with Figs. 12a and 13a. The massive changes are obvious: Partial destruction of capillaries; fragmentation of erythrocytes (EC'); accumulation of thrombocytes; formation of interstitial fibrin threads. Epithelial covering seemingly intact. x 4'7oo.

Fig. 17 Alveolar capillary of B4 lung in phase of destruction. Endothelial lining desintegrates (EN'). Basement membrane appears intact. x 23'2oo.

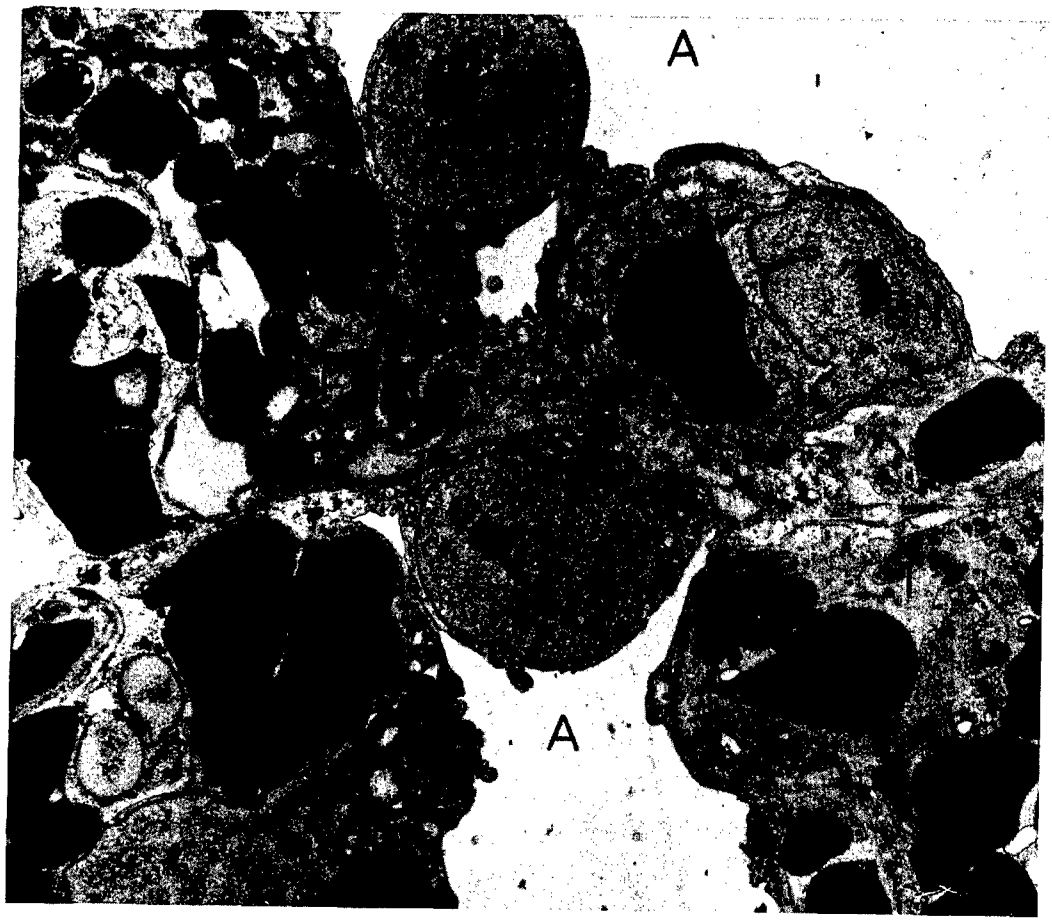

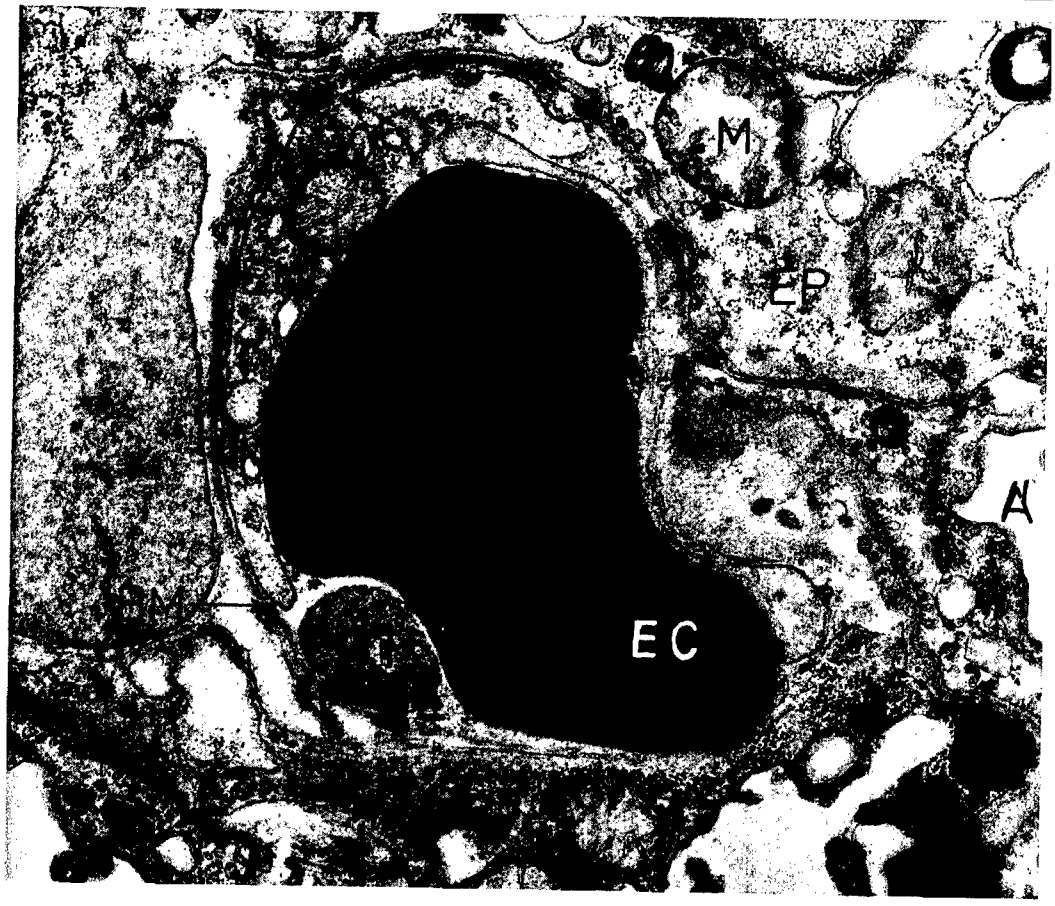

Figs. 16 (above) and 17 (below)

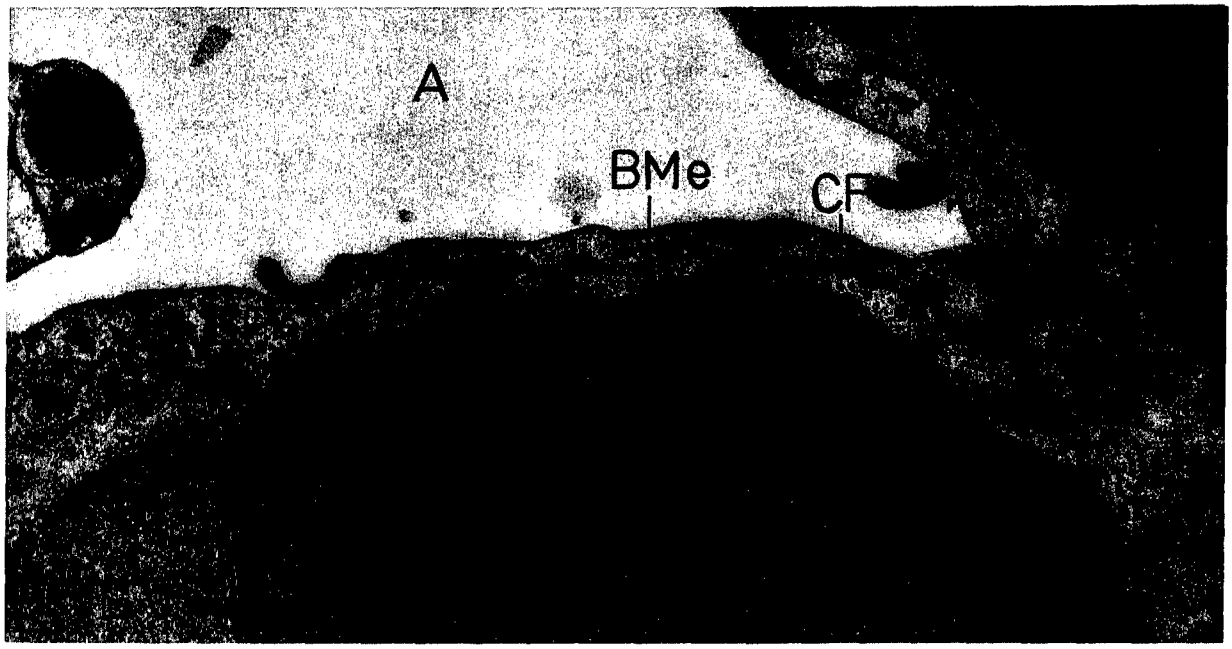

Fig. 18 Alveolo-capillary barrier of B4 lung. Endothelial lining is missing; erythrocyte cell membrane (arrows) touches basement membrane of former endothelium (BMe). Note difference in darkness of erythrocytes, indicating different hemoglobin density. x 24'2oo.

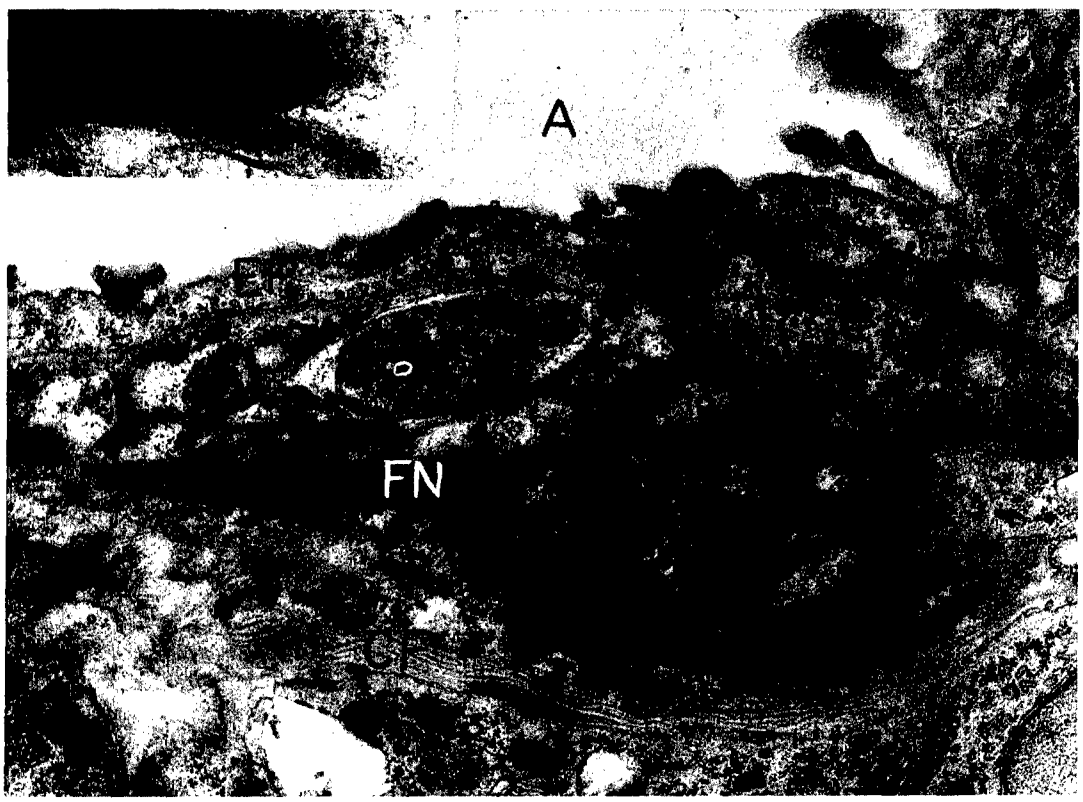

Fig. 19 Interstitial formation of fibrin in B4 lung. Insert demonstrates typical periodicity of fibrin filaments. x 17'5oo (insert x 57'ooo).

leucocytes and lymphocytes, by fragments of (destroyed) cells, and by thrombocytes and fibrin strands. Fig. 19 illustrates such a region, the fibrin nature of the dark staining strands being demonstrated by the characteristic periodicity observed at high power in the insert. It is interesting to note that the alveolar epithelium is usually found to be intact in these cases, even where the alveolus is filled with exudate.

Figs. 2o and 21 finally illustrate the three types of formed elements found in alveolar exudate in B4 lungs. The fibrin strands have been mentioned in relation to Figs. 7 and 11. Fig. 21 shows sections of such strands at high power, proving their fibrin

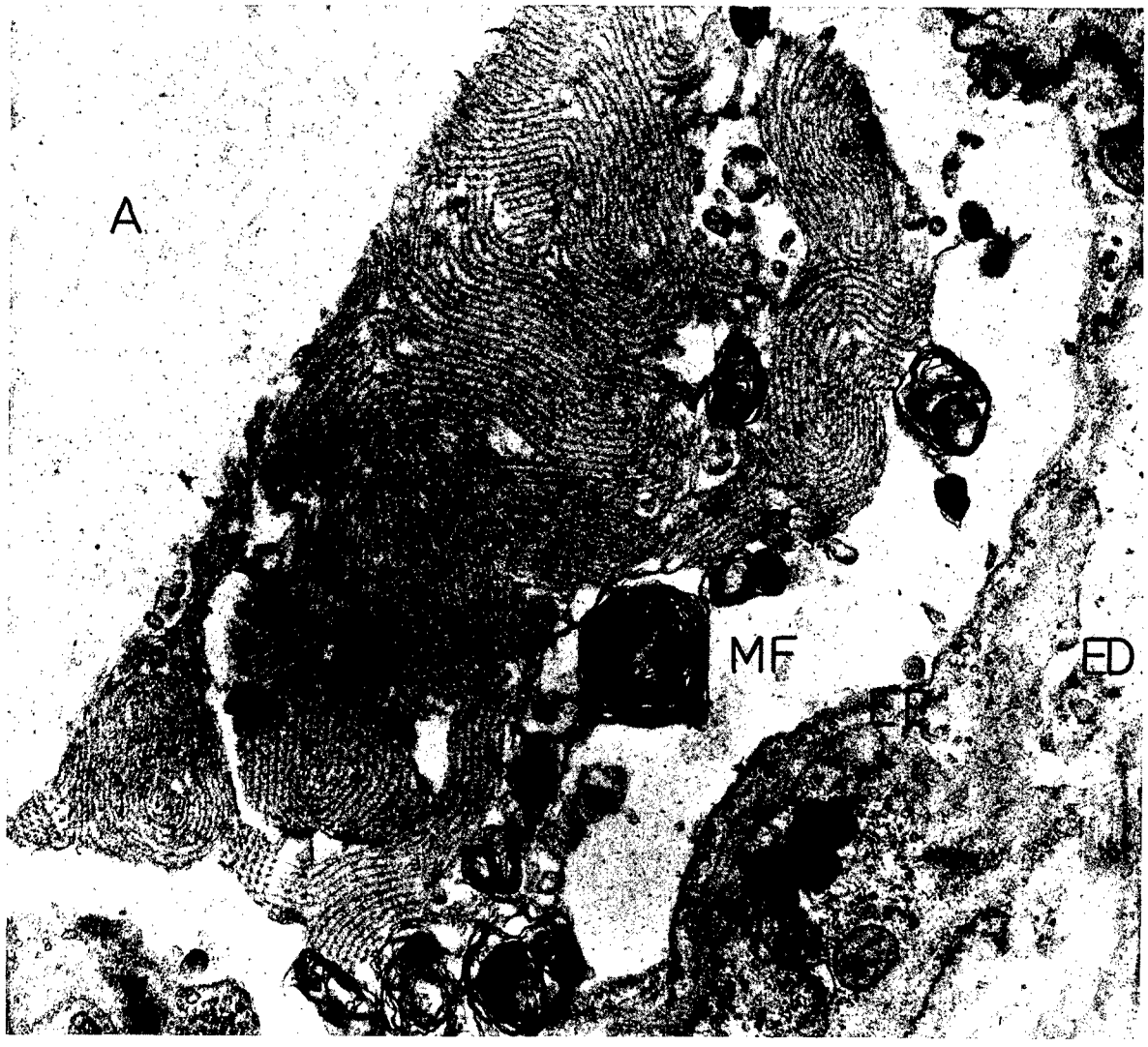

Fig. 2o Structure of formed components of alveolar exudate in B4 lung. Numerous "myelin figures" (i.e. concentric arrangement of strongly osmiophilic lamellae), and layered material of unidentified nature. x 24'2oo.

Fig. 21 Higher magnification of a "myelin figure" from alveolar exudate in B4 lung. Longitudinal sections of thread-like material shows periodicity characteristic of fibrin. x 42'8oo.

nature by the characteristic periodicity observed in the longitudinal sections. In addition, we found numerous spherical elements of varying size composed of concentric lamellae (Figs. 2o and 21). It is probable that these "myelin figures" consist of lipids. Another peculiar formed element of alveolar exudate was commonly observed: It consisted of "whorls" of subunits which were grouped in parallel and were clearly delineated by fine dark lines.Between these "lines" a pair of lighter lines was observed. The exact structure of this interesting material needs to be further investigated; its nature is unknown as yet.

B. Morphometric studies.

1) Over-all lung volume.

As base line values for the quantitative studies, the volumes of the inflated lungs were measured by fluid displacement after fixation in glutaraldehyde. The mean volumes of those lungs used in this study are given in table II. In all calculations of over-all parameters presented below, however, the individual lung volumes were used.

Table II:
Average volumes (V_L) of fixed lungs in ml. and lung volume-to-body weight ratios (V_L/BW) of rats used for quantitative study.

Group	V_L (mean)	V_L/ BW
CB	5,62 ± 0.60	0.045
B1	5.22 ± 0.74	0.045
B2	6.38 ± 0.41	0.054
B3	6.62 + 0.37	0.054
B4	4.42 ± 0.33	0.043

± values = S.D.

2) Morphometric survey of histologic sections in the light microscope

As discussed above, the light microscope allowed only a coarse evaluation of the damage to alveoli, while changes in capillary bed and tissue could not be reliably assessed because of the interfering section thickness. We have therefore restricted ourselves to a determination of the volume fraction of the lung occluded by alveolar exudate in the lungs of the B4 group as compared to the control group. The results are given in table III and in Fig. 22. It can be seen that, after 72 hours of exposure to O_2, 2/3 of the alveolar space is obliterated by exudate, almost half of which contains fibrin. This means that only 1/3 of the alveoli is, at best, available for gas exchange. These data have not been corrected for the effect of section thickness which leads to a systematic overestimation of the "dark" parts of the sections, i.e. the septa, by a factor of 2 to 3, with a corresponding underestimation of the alveolar space. For purposes of comparison this correction is not necessary. An extension of this survey to earlier stages appeared useless, because of the limited resolution attainable by this method.

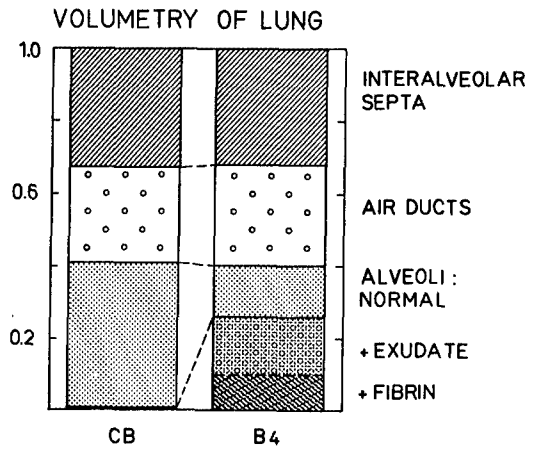

Fig. 22:
Comparison of composition of lung in control and B4 animals, obtained from light microscopy. Data not corrected for effect of section thickness!

Table III

Components	CB	B4
Septa	.33*	.31*
± S.E.	.006	.014
Ductuli	.26*	.28*
± S.E.	.016	.026
Alveoli	.41*	.41*
± S.E.	.010	.027
normal Alveoli	1.0	.35
obliterated Alv.	-	.65
± S.E.		.005
(Alv. containing	-	(.26)
Fibrin) ± S.E.		(.005)

* not corrected for section thickness effect!

3) Morphometric studies in the electron microscope.

The high resolution attainable by electron microscopy made it possible to investigate a considerable number of parameters. These can be classed into volume ratios, absolute volumes, surface areas,

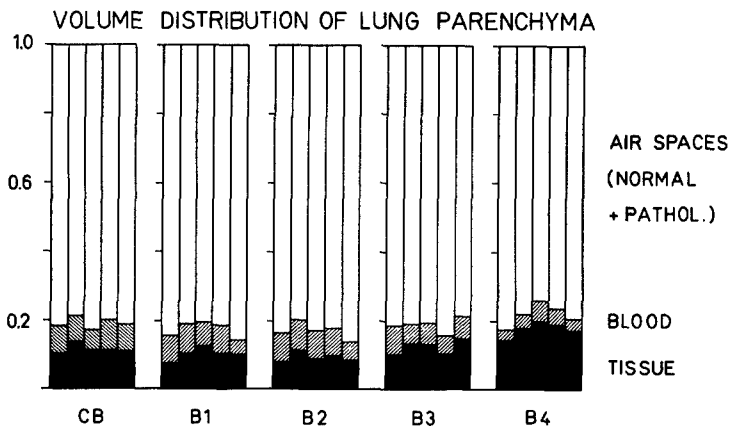

Fig. 23: Comparison of composition of lung obtained from electron microscopy.

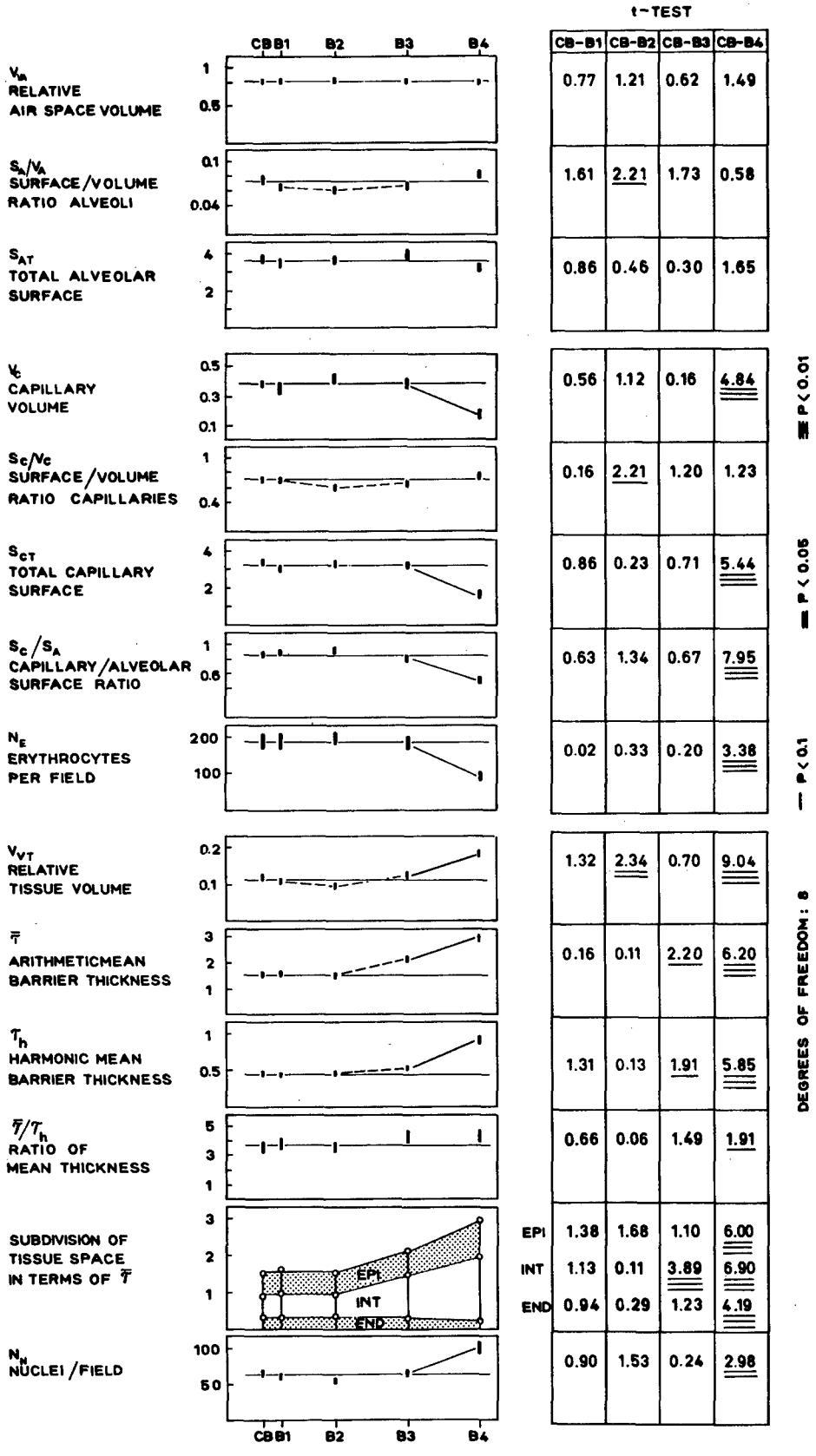

Fig. 24: Synopsis of results of morphometric study.

GROUP	V_{VA}	S_V/V_A	S_{AT}	V_C	S_C/V_C	S_{CT}	S_C/S_A	n_E	V_{VT}	$\bar{\tau}$	τ_h	$\bar{\tau}/\tau_h$	$\bar{\tau}_{EPI}$	$\bar{\tau}_{INT}$	$\bar{\tau}_{END}$	n_N
		μ^{-1}	10^3 cm^2	ml	μ^{-1}	10^3 cm^2				μ	μ		μ	μ	μ	
CB	.81	.077	3.82	.38	.70	3.40	.85	186	.117	1.51	.45	3.5	.67	.55	.29	66
± SE	.010	.005	.32	.039	.037	.26	.002	27.0	.006	.11	.017	.29	.032	.036	.017	4.4
B1	.82	.067	3.42	.35	.69	3.04	.88	186	.104	1.55	.42	3.8	.58	.71	.27	60
± SE	.013	.004	.29	.049	.053	.33	.044	24	.008	.16	.006	.40	.007	.138	.014	5.8
B2	.83	.060	3.64	.44	.59	3.33	.90	197	.094	1.50	.44	3.5	.60	.54	.28	54
± SE	.012	.006	.21	.039	.037	.195	.035	21	.008	.16	.017	.16	.030	.027	.017	6.5
B3	.81	.064	3.95	.39	.64	3.16	.81	179	.125	2.05	.51	4.2	.62	1.18	.25	64
±SE	.012	.006	.31	.033	.035	.210	.053	21	.010	.27	.025	.43	.039	.159	.026	7.0
B4	.78	.082	3.20	.17	.76	1.68	.52	92	.179	2.88	.90	4.3	.99	1.71	.18	102
± SE	.018	.007	.20	.019	.035	.18	.036	7	.003	.26	.075	.39	.061	.165	.020	11.2

Table IV: Synopsis of results

volume-to-surface ratios, thicknesses, and numbers of structures. The data resulting from this study are summarized in table IV and in Figs. 23 and 24. The results of the statistical tests are summarized in Fig. 24.

In Fig. 23 the over-all subdivision of the lung parenchyma into air spaces (normal and pathologic pooled), blood in capillaries, and tissue is histographically represented for each animal investigated. It illustrates the consistency of the data obtained on these minute random samples of tissue (see above).

a. Air spaces

In the normal lungs, and in those of the experimental groups B1 - B3 the air spaces occupied about 80 % of the lung volume (V_{VA} Table IV), the standard error being of the order of 1 %. In the B4 group the air space volume showed a tendency to drop; however the difference to the control values was not significant in the t-test (Fig. 24).

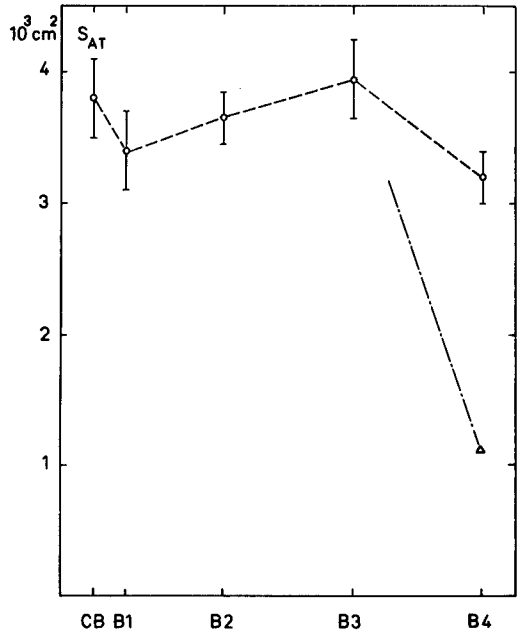

Fig. 25: Surface area of alveolar epithelium. (Triangle indicates alveolar surface area available for gas exchange in B4 lungs.)

The surface area of the alveolar epithelium S_{AT} showed much the same behavior (Fig. 25). It measured about 0.35 m^2. The small reduction in the B4 group was not significant. The alveolar surface-to-volume ratio (S_A/V_A) remained unchanged throughout, except for an unexplained slight drop in B2 (Fig. 24). From these data it can be concluded that the architectural framework of the lung remained unchanged despite the drastic formation of alveolar exudate.

b. Alveolar capillaries.

The capillary bed occupied 7 - 8 % of the total lung volume in groups CB, B1, B2 and B3 which amounted to an absolute volume (V_C) of approximately o.4 ml on the average, the standard error being of the order of 1o % (Fig. 26). In B4 V_C dropped to less than half, the difference being highly significant ($P < o.o1$). A concurrent observation related to the number of erythrocyte sections counted per field of observation (Fig. 27); the drop in B4 was again highly significant.

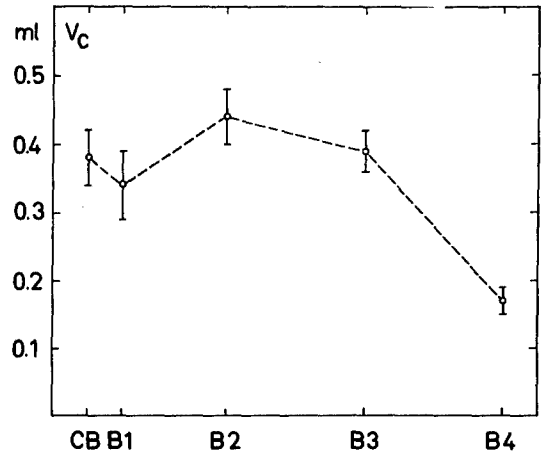

Fig. 26: Capillary volume.

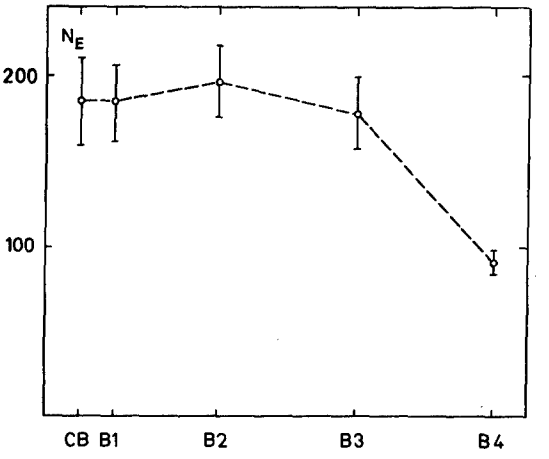

Fig. 27: Erythrocytes per field.

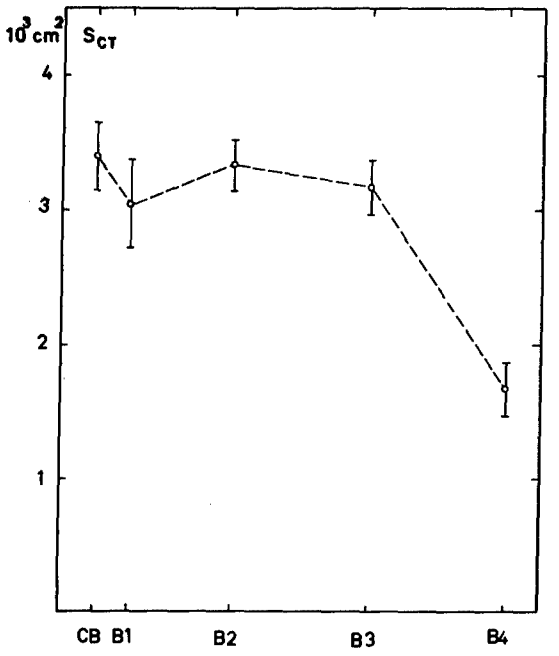

Fig. 28: Surface of capillary endothelium.

The total capillary surface area S_{CT} also fell from about o.3 m^2 in groups CB to B3 to about half in B4 (Fig. 28). But again the surface-to-volume ratio S_C/V_C remained constant (Fig. 24), indicating that the reduction of V_C and S_{CT} was due to a loss in the number of patent capillaries without much change in the general architecture of the remaining capillaries. The drop of this ratio in B2, which is slightly significant, cannot be explained and has to be further evaluated.

c. Alveolo-capillary tissue.

About 12 % of the total volume of control lungs is occupied by tissue (Fig. 24 and table IV). We observed a small decrease of this relative tissue volume V_{VT} in B2 ($P < o.o5$). In B3 V_{VT} is back to 12.5 % and climbs to 18 % in B4. The average thickness of the alveolo-capillary tissue barrier $\bar{\tau}$ was estimated at 1.5 μ with a standard error of o.15 μ (Fig. 29). It remained constant from CB to B2. The rise of $\bar{\tau}$ to 2.o5 μ observed in B3 was statistically significant at the level $P < o.1$. The further thickening of the barrier to $\bar{\tau}$ = 2.9 μ in B4 was however statistically highly significant ($P < o.ol$). We can therefore conclude that the tissue mass of the barrier becomes almost doubled after 72 hours in oxygen.

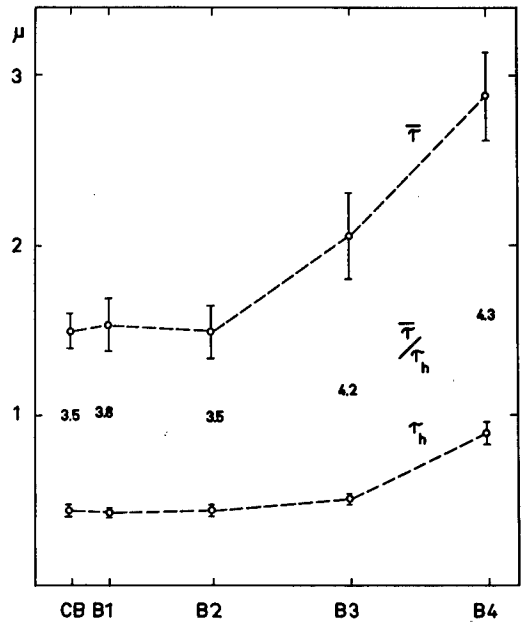

Fig. 29: Plot of arithmetic mean ($\bar{\tau}$) and harmonic mean ($\bar{\tau}_h$) of barrier thickness.

The effective thickness with respect to diffusion of gases between air and blood is however measured by the harmonic mean thickness τ_h estimated at o.45 μ in the control lungs (Fig. 29). τ_h remained unchanged in B1 and B2, showed a slight increase to o.51 μ in B3 ($P > o.1$), and a highly significant doubling to o.9 μ in B4 ($P > o.ol$).

It is thus interesting to note that arithmetic and harmonic mean thicknesses increased in parallel; there was only a slightly significant variation in the ratio of these two means $\bar{\tau}/\tau_h$ (Figs. 24 and 29). This ratio estimates the relative frequency of "thin" and "thick" regions of the barrier, in other words, it is a measure of its geometric configuration as a "rippled" membrane.

We were, then, interested to see how the different components of the tissue space were affected by the damage due to oxygen exposure, and have therefore calculated the mean thickness of alveolar epithelium, interstitium and capillary endothelium. The data obtained are listed in table IV and plotted in Fig. 3o. We note no changes in groups B1 and B2 with respect to the controls. At 48 hours (B3) the thickness of the interstitium is doubled ($P > o.ol$), while epithelium

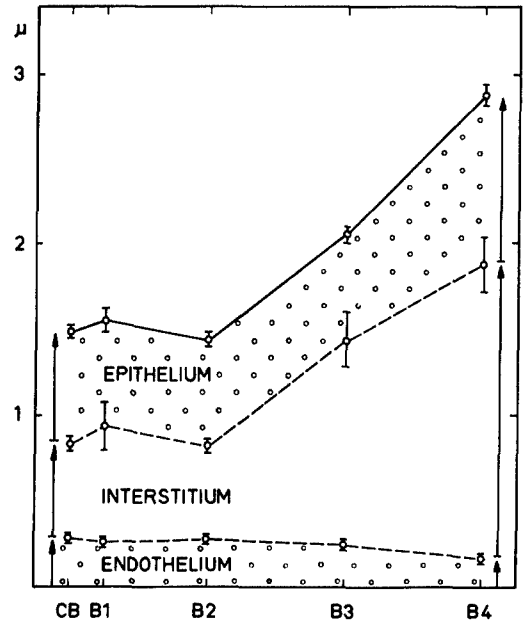

Fig. 30: Distribution of barrier thickness among components.

and endothelium preserve their original thickness. In the terminal B4 group the epithelium becomes thicker by 5o %, the interstitium shows a further increase to the triple of the control value, while the average thickness of the endothelium drops to 6o %. All these changes are significant at the $P > o.ol$ level.

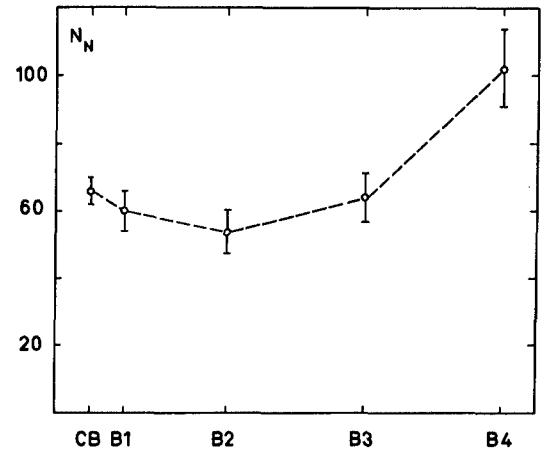

Fig. 31: Nuclei per field.

The average number n_N of sections through cell nuclei counted per field of observation (Fig. 31), showed a significant increase only in the B4 group. This could be related to two observed changes: The accumulation of leucocytes in the interstitium and the increase in the number of free alveolar cells (macrophages).

V. DISCUSSION

The phenomenological description of the pulmonary pathology observed in our experiments after prolonged exposure of rats to pure oxygen at atmospheric pressure in general confirms the findings of previous investigators, at least as far as conventional light microscopy is concerned. With respect to the ultrastructure of the damages, our findings differ in some points from those of Cedergren et al. (14). We could not find any "edematous swelling" of alveolar epithelial and capillary endothelial cells, as described by these investigators. The alveolar epithelium remained astoundingly unchanged and exhibited, on quantitative analysis, a slight thickening only in the terminal phase. From the appearance of the epithelial cells we would tend to typify this thickening rather as proliferation than as cytoplasmic swelling. The cytoplasmic changes accompanying the disintegration of the capillary endothelial lining were in many respects also different from simple "cytoplasmic edema". In the development of extensive interstitial edema during the second day (B3, Figs. 13-14) the fluid accumulated clearly within the interstitial ground substance space. The basement membranes remained closely apposed to endothelial and epithelial cells. Some of these differences may be due to the different methods of preparation used here as compared to the earlier work of Cedergren et al. In the other points our observations agree, particularly with respect to the occurence of mitochondrial swelling in alveolar epithelial cells, which we also found to be not too frequent, and only appearing in the terminal stages. This in contrast to Schulz (22) who described this phenomenon as a characteristic cellular lesion of oxygen toxicity. This point will be further investigated.

This study pursued two chief aims: (1) a definition of the time sequence of events, and (2) a quantitative definition of the degree and extent of damage, with the goal of possibly defining the degree of impairment of lung function.

Time sequence of events.

The first detectable damage of the lung occurs during the second day of exposure to O_2, beginning with interstitial edema, probably due to a gradual development of defects in the capillary endothelial lining. The tissue space also becomes infiltrated by leucocytes and thrombocytes; fibrin forms interstitially. During the third day this damage becomes precipitously aggravated, with an appreciable destruction of capillaries accompanied by destruction of numerous erythrocytes. During this third day a profuse exudation must take place into a large fraction of alveoli. They become completely filled with a fluid containing numerous macrophages, erythrocytes, leucocytes, cell debris, fibrin strands, lipids and some unidentidied organized material which possibly is a protein-lipid-compound.

This appears as the terminal stage, reached for rats after 72 hours in O_2, at which survival in room air is no longer possible; even in a high oxygen atmosphere the animals rapidly die.

It thus appears, that the basic toxic effect of oxygen must be initiated rather early, that is towards the end of the first day of exposure, since all the observed effects must be secondary to some still unknown disturbance at the subcellular - or even molecular - level.

Quantitative definition of damage.

Hitherto, no attempt at quantitative evaluation of pulmonary pathology due to oxygen poisoning has been attempted, although some quantitative statements have been expressed on the basis of mere subjective observation. The application of established morphometric techniques (23, 24, 29 - 34) has allowed an objective quantitative appreciation of the damages, which could be statistically evaluated. This can be summarized as follows (compare Fig.24):

a. Air spaces. The architectural framework of the air spaces remains unchanged. However, during the third day up to 65 % of the alveoli become obliterated by exudate and are thus eliminated as gas exchange units. Only 35 % of the measured surface of the aveolar epithelium remains available for gas exchange (Fig. 25).

b. Capillaries. Volume and surface of the alveolar capillaries remain constant for the first two days, but become significantly reduced during the third day. At no point is there an increase of either capillary volume or surface (or of the capillary endothelial volume) which could indicate a general enlargement of capillaries (1), or even a capillary proliferation as suggested by Pratt (21) for humans. During the second and third day there is even a gradual but extensive destruction of capillaries, correlating to the drop in V_C.

The slightly significant reduction in the ratio S_C/V_C after one day in O_2 (Fig. 24) may be related to the observation of irregular size of the capillaries. With a widening of the distribution of capillary diameters the total capillary surface would tend to fall if the over-all volume remained constant. Some scattered dilated capillaries might also appear as congestion or even proliferation, mainly in thick histologic preparations.

c. Alveolo-capillary barrier. The average thickness $\bar{\tau}$ of the alveolo-capillary barrier, which includes alveolar epithelium, interstitium, and capillary endothelium, measures the mass of tissue separating air and blood. Functionally however, the harmonic mean thickness τ_h is the over-all measure of resistance to gas exchange (29). Both these dimensions show a concurrent slight increase during the second day which is most severely aggravated during the third day. $\bar{\tau}$ rises from normally 1.5 μ to 3 μ after 72 hours;

τ_h from 0.45 μ in the controls to 0.9 μ in the terminal stage. This increase in thickening is restricted to a widening of the interstitial space during the second day. During the third day the epithelium also becomes significantly thickened; the interstitium enlarges still more, while the endothelium is reduced by regional destruction.

Effect of these changes on lung function.

Studies in men breathing oxygen under the same conditions as those of the present study showed a drop in diffusing capacity to 81% of the control value after 48 hours and to 73% after 74 hours of exposure. The total lung capacity fell to 72% of the control value after 74 hours (7). These results might readily be explained on the basis of thickening of the air-blood tissue barrier, a decrease in pulmonary capillary surface area and alveolar edema formation seen in the present study.

Since, in the experiments reported here, principal structural elements related to the diffusing capacity of the air-blood barrier could be measured, it was possible to make an estimate of its capacity for gas exchange from the proportionality relationship:

$$D_m \propto \frac{S_{CT}}{\tau_h}$$

where, D_m is the gas exchange capacity of the air-blood tissue barrier, S_{CT} is the capillary surface area, and τ_h is the harmonic mean thickness of the air-blood tissue barrier.

The results, expressed as percent of control value, indicate a fall of the air-blood barrier diffusing capacity to 25% after 72 hours of oxygen exposure (Table V and Fig.32). Taking into consideration the obliteration by edema of 65% of the functional air units at 72 hours, the estimated diffusing capacity fell to 9% of the control value (Closed Circle on Fig. 32).

	Time of exposure to 98.5% oxygen (hours)				
	0	6	24	48	72
S_{AT} (m^2)	.38	.34	.36	.39	.32
S_{CT} (m^2)	.34	.30	.33	.32	.17*
τ_h (μ)	.45	.42	.44	.51	.90*
$\frac{D_m \text{ test}}{D_m \text{ control}}$ (%)	100	95	99	83	25

Table V:

Total alveolar surface (S_{AT}), total capillary surface(S_{CT}), harmonic mean barrier thickness (τ_h) and air-blood barrier diffusing capacity (D_m) of the test groups, expressed as percent of the control value.

* $p<0.01$

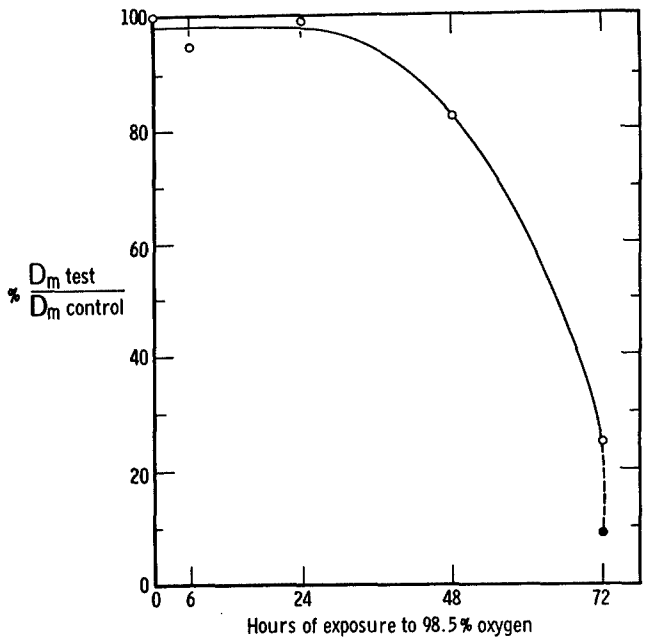

Fig. 32: Diffusing capacities.

Air-blood barrier diffusing capacity (D_m) of the test groups, expressed in percent of the control value (see text).

VI. CONCLUSIONS

The primary site of damage caused by pure oxygen breathing at 765 Torr appeared to be in the endothelial cells of the pulmonary capillaries with resultant movement of fluid into the interstitial and alveolar spaces.

After 72 hours of oxygen exposure, the alveolo-capillary tissue barrier had doubled in thickness, the capillary bed was reduced in volume by about one half, and a profuse exudate containing numerous cells had covered about 65 percent of the alveolar surface. These factors combined to progressively reduce the estimated diffusing capacity of the air-blood barrier to about 9 percent of its normal value.

REFERENCES

1. Roth, E. M., Space Cabin Atmospheres, Part I. Oxygen Toxicity, NASA SP-47.

2. Becker-Freyseng, H., and H. G. Clamann, German Aviation Medicine in World War II, Vol 1, pp 493-514, 1950.

3. Clamann, H. G., and H. Becker-Freyseng, Luftfahrtmedizin Vol 4, p 1, 1939.

4. Comroe, J. H., R. D. Dripps, P. R. Dumke, and M. Deming, J.A.M.A., Vol 128, p 710, 1945.

5. Ohlsson, W. T. L., Acta Med. Scand., Suppl. 190, pp 1-93, 1947.

6. Welch, B. E., T. E. Morgan, F. Ulvedal, and W. W. Henderson, Aero space Med., Vol 32, p 7, p 583, p 591, p 603, p 610, 1961.

7. Caldwell, P.R.B., W.L. Lee, Jr., H.S. Schildkraut and E.R. Archibald. J. Appl. Physiol. in press. 1966.

8. Ernsting, J., J. Physiol., Vol 155, p 51, 1961.

9. Campbell, J. A., J. Physiol., Vol 63, p 325, 1927.

10. Helvey, W. M., Final Report, RAC 393-1, ARD 807-701, Republic Aviation Corp., 1962.

11. Cook, S. F., and H. F. Leon, AFMDC-TR-60-21, Holloman Air Force Base, New Mexico, 1960.

12. Penrod, K. E., Final Report, Contract NONR 473(00), 1959, (AD No. 218 094).

13. Caldwell, P. R. B., S. T. Giammona, W. L. Lee, and S. Bondurant, Ann. N.Y. Acad. Sci., Vol 121, p 823, 1965.

14. Cedergren, B., L. Gyllensten, and J. Wersall, Acta Pediat., Vol 48, p 477, 1959.

15. Mac Hattie, L. and H. Rahn, Proc. Soc. Exp. Med. Biol., Vol 104, p 772, 1960.

16. Clamann, H. G., H. Becker-Freyseng, and G. Liebegott, Luftfahrtmedizin, Vol 5, p 17, 1941.

17. Pichotka, J., Beitr.z.path.Anat. u.z. allg.Path., Vol 105, p 381, 1941.

18. Liebegott, G., Beitr.z.path.Anat. u.z. allg.Path., Vol 105, p 413, 1941.

19. Paine, J. R., D. Lynn, and A. Keys, Amer. J. Physiol., Vol 133, p 406, 1941.

20. Weir, F. W., D. W. Bath, P. Yevich, and F. W. Oberst, A Study on the Effects of Continuous Inhalation of High Concentrations of Oxygen at Ambient Pressure and Temperature, ASD-TR-61-664, Aeronautical Systems Division, Wright-Patterson Air Force Base, Ohio, 1961.

21. Pratt, P.C., Ann. N.Y. Acad. Sci., Vol 121, p 809, 1965.

22. Schulz, H., Die Naturwissenschaften, Vol 9, p 205, 1956.

23. Weibel, E. R., Morphometry of the Lung, Springer, Heidelberg, 1963.

24. Weibel, E. R., Handbook of Physiology, Section 3, Vol 1, p 285, 1964.

25. Byers, D. H., and B. E. Saltzman, Am. Ind. Hyg. Assoc. J., Vol 19, p 251, 1958.

26. Thorp, C. E., Armour Research Foundation, pp 118-119, 1955.

27. Luft, J. H., J. Biophys. Biochem. Cytol., Vol 9, p 409, 1961.

28. Reynolds, E. S., J. Cell Biol., Vol 17, p 208, 1963.

29. Weibel, E. R., and B. W. Knight, J. Cell Biol., Vol 21, pp 367-384, 1964.

30. Weibel, E. R., Lab. Invest., Vol 12, p 131, 1963.

31. Hennig, A., Z.wiss.Mikr., Vol 63, pp 67-71, 1956.

32. Hennig, A., Mikroskopie, Vol 11, pp 1-20, 1956.

33. Chalkley, H. W., J. Cornfield, and H. Park, Science, Vol 110, p 295, 1949.

34. Weibel, E. R., and D. M. Gomez, J. Appl. Physiol., Vol 17, pp 343-348, 1962.

Security Classification

DOCUMENT CONTROL DATA - R&D

(Security classification of title, body of abstract and indexing annotation must be entered when the overall report is classified)

1. ORIGINATING ACTIVITY (Corporate author)	2a. REPORT SECURITY CLASSIFICATION
University of Zurich Dept of Anatomy Zurich, Switzerland	UNCLASSIFIED
	2b GROUP N/A

3. REPORT TITLE

ELECTRON MICROSCOPIC AND MORPHOMETRIC STUDY OF RATS EXPOSED TO 98.5 PERCENT OXYGEN AT ATMOSPHERIC PRESSURE

4. DESCRIPTIVE NOTES *(Type of report and inclusive dates)*

Final report, February 1964 - July 1965

5. AUTHOR(S) *(Last name, first name, initial)*

Kistler, Gonzague S., MD
Caldwell, Peter R.B., Captain, MC, USAF
Weibel, Ewald R., MD

6. REPORT DATE	7a. TOTAL NO. OF PAGES	7b. NO. OF REFS
December 1965	40	35

8a. CONTRACT OR GRANT NO.	9a. ORIGINATOR'S REPORT NUMBER(S)
AF 61(052)-784	
b. PROJECT NO 7164	
c. Task No. 716404	9b. OTHER REPORT NO(S) *(Any other numbers that may be assigned this report)*
d.	AMRL-TR-65-66

10. AVAILABILITY/LIMITATION NOTICES

Distribution of this document is unlimited.

11. SUPPLEMENTARY NOTES	12 SPONSORING MILITARY ACTIVITY
	Aerospace Medical Research Laboratories, Aerospace Medical Div., Air Force Systems Command, Wright-Patterson AFB, Ohio

13. ABSTRACT

Rats were exposed to 98.5% oxygen at 765 Torr in a controlled environmental chamber. Groups were sacrificed at 6, 24, 48, and 72 hours and the lungs were prepared for light and electron microscopic examination. A control group breathed room air. In the groups which breathed oxygen for 6 and 24 hours no changes in lung structure could be observed. After 48 hours the interstitial space was enlarged by accumulation of fluid and early destructive changes of the capillary endothelial lining were found. After 72 hours the widened interstitial space contained numerous leucocytes, thrombocytes and other cells; fibrin strands were numerous. There was marked destruction of the pulmonary capillaries. At this stage, 65% of all alveoli were filled with an exudate containing leucocytes, erythrocytes, macrophages and fibrin strands. There was a decrease in capillary blood volume and of endothelial surface after 72 hours. The thickness of the air-blood barrier was increased after 48 and doubled after 72 hours. The barrier thickening was mainly due to increase of the interstitial space; terminally, the epithelium was also thickened, although the endothelium became thinner, on the average, due to destruction. As a result of these alterations there was a marked fall in estimated gas exchange capacity of the air-blood tissue barrier.

DD FORM 1 JAN 64 1473

AF-WP-B-AUG 64 400

Security Classification

14. KEY WORDS	LINK A		LINK B		LINK C	
	ROLE	WT	ROLE	WT	ROLE	WT
Pulmonary pathology Oxygen toxicity Rats Electron microscophy Morphometric methods						

INSTRUCTIONS

1. ORIGINATING ACTIVITY: Enter the name and address of the contractor, subcontractor, grantee, Department of Defense activity or other organization *(corporate author)* issuing the report.

2*a*. REPORT SECURITY CLASSIFICATION: Enter the overall security classification of the report. Indicate whether "Restricted Data" is included. Marking is to be in accordance with appropriate security regulations.

2*b*. GROUP: Automatic downgrading is specified in DoD Directive 5200.10 and Armed Forces Industrial Manual. Enter the group number. Also, when applicable, show that optional markings have been used for Group 3 and Group 4 as authorized.

3. REPORT TITLE: Enter the complete report title in all capital letters. Titles in all cases should be unclassified. If a meaningful title cannot be selected without classification, show title classification in all capitals in parenthesis immediately following the title.

4. DESCRIPTIVE NOTES: If appropriate, enter the type of report, e.g., interim, progress, summary, annual, or final. Give the inclusive dates when a specific reporting period is covered.

5. AUTHOR(S): Enter the name(s) of author(s) as shown on or in the report. Enter last name, first name, middle initial. If military, show rank and branch of service. The name of the principal author is an absolute minimum requirement.

6. REPORT DATE: Enter the date of the report as day, month, year; or month, year. If more than one date appears on the report, use date of publication.

7*a*. TOTAL NUMBER OF PAGES: The total page count should follow normal pagination procedures, i.e., enter the number of pages containing information.

7*b*. NUMBER OF REFERENCES: Enter the total number of references cited in the report.

8*a*. CONTRACT OR GRANT NUMBER: If appropriate, enter the applicable number of the contract or grant under which the report was written.

8*b*, 8*c*, & 8*d*. PROJECT NUMBER: Enter the appropriate military department identification, such as project number, subproject number, system numbers, task number, etc.

9*a*. ORIGINATOR'S REPORT NUMBER(S): Enter the official report number by which the document will be identified and controlled by the originating activity. This number must be unique to this report.

9*b*. OTHER REPORT NUMBER(S): If the report has been assigned any other report numbers *(either by the originator or by the sponsor)*, also enter this number(s).

10. AVAILABILITY/LIMITATION NOTICES: Enter any limitations on further dissemination of the report, other than those imposed by security classification, using standard statements such as:

(1) "Qualified requesters may obtain copies of this report from DDC."

(2) "Foreign announcement and dissemination of this report by DDC is not authorized."

(3) "U. S. Government agencies may obtain copies of this report directly from DDC. Other qualified DDC users shall request through

_____."

(4) "U. S. military agencies may obtain copies of this report directly from DDC. Other qualified users shall request through

_____."

(5) "All distribution of this report is controlled. Qualified DDC users shall request through

_____."

If the report has been furnished to the Office of Technical Services, Department of Commerce, for sale to the public, indicate this fact and enter the price, if known.

11. SUPPLEMENTARY NOTES: Use for additional explanatory notes.

12. SPONSORING MILITARY ACTIVITY: Enter the name of the departmental project office or laboratory sponsoring *(paying for)* the research and development. Include address.

13. ABSTRACT: Enter an abstract giving a brief and factual summary of the document indicative of the report, even though it may also appear elsewhere in the body of the technical report. If additional space is required, a continuation sheet shall be attached.

It is highly desirable that the abstract of classified reports be unclassified. Each paragraph of the abstract shall end with an indication of the military security classification of the information in the paragraph, represented as *(TS), (S), (C), or (U)*

There is no limitation on the length of the abstract. However, the suggested length is from 150 to 225 words.

14. KEY WORDS: Key words are technically meaningful terms or short phrases that characterize a report and may be used as index entries for cataloging the report. Key words must be selected so that no security classification is required. Identifiers, such as equipment model designation, trade name, military project code name, geographic location, may be used as key words but will be followed by an indication of technical context. The assignment of links, rules, and weights is optional.

NOTICES

When US Government drawings, specifications, or other data are used for any purpose other than a definitely related Government procurement operation, the Government thereby incurs no responsibility nor any obligation whatsoever, and the fact that the Government may have formulated, furnished, or in any way supplied the said drawings, specifications, or other data, is not to be regarded by implication or otherwise, as in any manner licensing the holder or any other person or corporation, or conveying any rights or permission to manufacture, use, or sell any patented invention that may in any way be related thereto.

Requests for copies of this report should be directed to either of the addressees listed below, as applicable:

Federal Government agencies and their contractors registered with Defense Documentation Center (DDC):

DDC
Cameron Station
Alexandria, Virginia 22314

Non-DDC users (stock quantities are available for sale from):

Chief, Input Section
Clearinghouse for Federal Scientific & Technical Information (CFSTI)
Sills Building
5285 Port Royal Road
Springfield, Virginia 22151

Change of Address

Organizations and individuals receiving reports via the Aerospace Medical Research Laboratories' automatic mailing lists should submit the addressograph plate stamp on the report envelope or refer to the code number when corresponding about change of address or cancellation.

Do not return this copy. Retain or destroy.

The experiments reported herein were conducted according to the "Principles of Laboratory Animal Care" established by the National Society for Medical Research.

700 - February 1966 - 773-32-657